

DAPNIA-02-380  
 LPT Orsay 02-122  
 LMU-02-19  
 PCCF-RI-0218  
 hep-ph/0301165

# Testing QCD factorisation and charming penguins in charmless $B \rightarrow PV$

R. Aleksan<sup>a\*</sup>, P.-F. Giraud<sup>a†</sup>, V. Morénas<sup>b‡</sup>, O. Pène<sup>c§</sup> and A. S. Safir<sup>d\*\*</sup>.

<sup>a</sup> CEA Saclay, DAPNIA/SPP (Bât. 141) F-91191 Gif-sur-Yvette CEDEX, France.

<sup>b</sup> LPC, Université Blaise Pascal - CNRS/IN2P3 F-63000 Aubière Cedex, France.

<sup>c</sup> LPT (Bât.210), Université de Paris XI, Centre d'Orsay, 91405 Orsay-Cedex, France.

<sup>d</sup> LMU München, Sektion Physik, Theresienstraße 37, D-80333 München, Germany.

November 1, 2018

We try a global fit of the experimental branching ratios and CP-asymmetries of the charmless  $B \rightarrow PV$  decays according to QCD factorisation. We find it impossible to reach a satisfactory agreement, the confidence level (CL) of the best fit is smaller than .1 %. The main reason for this failure is the difficulty to accomodate several large experimental branching ratios of the strange channels. Furthermore, experiment was not able to exclude a large direct CP asymmetry in  $\overline{B^0} \rightarrow \rho^+ \pi^-$ , which is predicted very small by QCD factorisation. Trying a fit with QCD factorisation complemented by a charming-penguin inspired model we reach a best fit which is not excluded by experiment (CL of about 8 %) but is not fully convincing. These negative results must be tempered by the remark that some of the experimental data used are recent and might still evolve significantly.

---

\*e-mail :aleksan@hep.saclay.cea.fr

†e-mail :giraudpf@hep.saclay.cea.fr

‡e-mail :morenas@clermont.in2p3.fr

§e-mail :pene@th.u-psud.fr

\*\*e-mail :safir@theorie.physik.uni-muenchen.de

## I. INTRODUCTION

It is an important theoretical challenge to master the non-leptonic decay amplitudes and particularly  $B$  non-leptonic decay. It is not only important *per se*, in view of the many experimental branching ratios which have been measured recently with increasing accuracy by BaBar [1–10], Belle [11–15] and CLEO [16–21], but it is also necessary in order to get control over the measurement of CP violating parameters and particularly the so-called angle  $\alpha$  of the unitarity triangle. It is well known that extracting  $\alpha$  from measured indirect CP asymmetries needs a sufficient control of the relative size of the so-called tree ( $T$ ) and penguins ( $P$ ) amplitudes.

However the theory of non-leptonic weak decays is a difficult issue. Lattice QCD gives predictions for semi-leptonic or purely leptonic decays but not directly for non-leptonic ones. Since long, one has used what is now called “naive factorization” which replaces the matrix element of a four-fermion operator in a heavy-quark decay by the product of the matrix elements of two currents, one semi-leptonic matrix element and one purely leptonic. For long it was noticed that naive factorization did provide reasonable results although it was impossible to derive it rigorously from QCD except in the  $N_c \rightarrow \infty$  limit. It was also well-known that the matrix elements computed via naive factorization have a wrong anomalous dimension.

Recently an important theoretical progress has been performed [22,23] which is commonly called “QCD factorisation”. It is based on the fact that the  $b$  quark is heavy compared to the intrinsic scale of strong interactions. This allows to deduce that non-leptonic decay amplitudes in the heavy-quark limit have a simple structure. It implies that corrections termed “non-factorizable”, which were thought to be intractable, can be calculated rigorously. The anomalous dimension of the matrix elements is now correct to the order at which the calculation is performed. Unluckily the subleading  $\mathcal{O}(\Lambda/m_b)$  contributions cannot in general be computed rigorously because of infrared singularities, and some of these which are chirally enhanced are not small, of order  $\mathcal{O}(m_\pi^2/m_b(m_u + m_d))$ , which shows that the inverse  $m_b$  power is compensated by  $m_\pi/(m_u + m_d)$ . In the seminal papers [22,23], these contributions are simply bounded according to a qualitative argument which could as well justify a significantly larger bound with the risk of seeing these unpredictable terms become dominant. It is then of utmost importance to check experimentally QCD factorisation.

Since a few years it has been applied to  $B \rightarrow PP$  (two charmless pseudoscalar mesons) decays. The general feature is that the decay to non-strange final states is predicted slightly larger than experiment while the decay to strange final states is significantly underestimated. In [23] it is claimed that this can be cured by a value of the unitarity-triangle angle  $\gamma$  larger than generally expected, larger maybe than 90 degrees. Taking also into account various uncertainties the authors conclude positively as for the agreement of QCD factorisation with the data. In [24,25] it was objected that the large branching ratios for strange channels argued in favor of the presence of a specific non perturbative contribution called “charming penguins” [25–30]. We will return to this approach later.

The  $B \rightarrow PV$  (charmless pseudoscalar + vector mesons) channels are more numerous and allow a more extensive check. In ref. [31] it was shown that naive factorisation implied a rather small  $|P|/|T|$  ratio, for  $B^0 \rightarrow \rho^\pm \pi^\mp$  decay channel, to be compared to the larger one for the  $B \rightarrow \pi^+ \pi^-$ . This prediction is still valid in QCD factorisation where the  $|P|/|T|$  ratio is of about 3 % (8 %) for the  $\overline{B^0} \rightarrow \rho^+ \pi^-$  ( $\overline{B^0} \rightarrow \rho^- \pi^+$ ) channel against about 20 % for the  $\overline{B^0} \rightarrow \pi^+ \pi^-$  one. If this prediction was reliable it would put the  $\overline{B^0} \rightarrow \rho^+ \pi^-$  channel in a good position to measure the CKM angle  $\alpha$  via indirect CP violation. This remark triggered the present work: we wanted to check QCD factorisation in the  $B \rightarrow PV$  sector to estimate the chances for a relatively easy determination of the angle  $\alpha$ .

The non-charmed  $B \rightarrow PV$  amplitudes have been computed in naive factorisation [32], in some extension of naive factorisation including strong phases [33], in QCD factorisation [34–36] and some of them in the so-called perturbative QCD [38,39]. In [41], a global fit to  $B \rightarrow PP, PV, VV$  was investigated using QCDF in the heavy quark limit and it has been found a plausible set of soft QCD parameters that apart from three pseudoscalar vector channels, fit well the experimental branching ratios. Recently [36] it was claimed from a global fit to  $B \rightarrow PP, PV$  that the predictions of QCD factorization are in good agreement with experiment when one excludes some channels from the global fit. When this paper appeared we had been for some time considering this question and our feeling was significantly less optimistic. This difference shows that the matter is far from trivial mainly because experimental uncertainties can still be open to some discussion. We would like in this paper to understand better the origin of the difference between our unpublished conclusion and the one presented in [36] and try to settle the present status of the comparison of QCD factorisation with experiment.

One general remark about QCD factorisation is that it yields predictions which do not differ so much from naive factorisation ones. This is expected since QCD factorisation makes a perturbative expansion the zeroth order of which being naive factorisation. As a consequence, QCD factorisation predicts very small direct CP violation in the non-strange channels. Naive factorisation predicts vanishing direct CP violation. Indeed, direct

CP violation needs the occurrence of two distinct strong contributions with a strong phase between them. It vanishes when the subdominant strong contribution vanishes and also when the relative strong phase does as is the case in naive factorisation. In the case of non-strange decays, the penguin ( $P$ ) and tree ( $T$ ) contributions being at the same order in Cabibbo angle, the penguin is strongly suppressed because the Wilson coefficients are suppressed by at least one power of the strong coupling constant  $\alpha_s$ , and the strong phase in QCD factorisation is generated by a  $\mathcal{O}(\alpha_s)$  corrections. Having both  $P/T$  and the strong phase small, the direct CP asymmetries are doubly suppressed. Therefore a sizable experimental direct CP asymmetry in  $\bar{B}^0 \rightarrow \rho^+ \pi^-$  which is not excluded by experiment [9] would be at odds with QCD factorisation. We will discuss this later on. Notice that this argument is independent of the value of the unitarity angle  $\gamma$ , contrarily to arguments based on the value of some branching ratios which depend on  $\gamma$  [23].

The Perturbative QCD (PQCD) predicts larger direct CP asymmetries than QCDF due to the fact that penguin contributions to annihilation diagrams, claimed to be calculable in PQCD, contribute to a larger amount to the amplitude and have a large strong phase. In fact, in PQCD, this penguin annihilation diagram is claimed to be of the same order,  $\mathcal{O}(\alpha_s)$ , than the dominant naive factorisation diagram while in QCDF it is also  $\mathcal{O}(\alpha_s)$  but smaller than the dominant naive factorisation which is  $\mathcal{O}(1)$ . Hence, in PQCD, this large penguin contribution with a large strong phase yields a large CP asymmetry [40,42,43].

If QCD factorisation is concluded to be unable to describe the present data satisfactorily, while there is to our knowledge no theoretical argument against it, we have to incriminate non-perturbative contributions which are larger than expected. One could simply enlarge the allowed bound for those contributions which are formally subleading but might be large. However a simple factor two on these bounds makes these unpredictable contributions comparable in size with the predictable ones, if not larger. This spoils the predictivity of the whole program.

A second line is to make some model about the non-perturbative contribution. The “charming penguin” approach [27,30] starts from noticing the underestimate of strange-channels branching ratios by the factorisation approaches. This will be shown to apply to the  $PV$  channels as well as to the  $PP$  ones. This has triggered us to try a charming-penguin inspired approach. It is assumed that some hadronic contribution to the penguin loop is non-perturbative. In other words that weak interactions create a charm-anticharm intermediate state which turns into non-charmed final states by strong rescattering. In order to make the model as predictive as possible we will use not more than two unknown complex numbers and use flavor symmetry in strong rescattering.

In section II we will recall the weak-interaction effective Hamiltonian. In section III we will recall QCD factorisation. In section IV we will compare QCD factorisation with experimental branching ratios and direct CP asymmetries. In section V we will propose a model for non-perturbative contribution and compare it to experiment. We will then conclude.

## II. THE EFFECTIVE HAMILTONIAN

The effective weak Hamiltonian for charmless hadronic  $B$  decays consists of a sum of local operators  $Q_i$  multiplied by short-distance coefficients  $C_i$  given in table I, and products of elements of the quark mixing matrix,  $\lambda_p = V_{pb}V_{ps}^*$  or  $\lambda'_p = V_{pb}V_{pd}^*$ . Below we will focus on  $B \rightarrow PV$  decays; where  $P$  and  $V$  hold for pseudoscalar and vector mesons respectively. Using the unitarity relation  $-\lambda_t = \lambda_u + \lambda_c$ , we write

$$\mathcal{H}_{\text{eff}} = \frac{G_F}{\sqrt{2}} \sum_{p=u,c} \lambda_p \left( C_1 Q_1^p + C_2 Q_2^p + \sum_{i=3,\dots,10} C_i Q_i + C_{7\gamma} Q_{7\gamma} + C_{8g} Q_{8g} \right) + \text{h.c.}, \quad (1)$$

where  $Q_{1,2}^p$  are the left-handed current-current operators arising from  $W$ -boson exchange,  $Q_{3,\dots,6}$  and  $Q_{7,\dots,10}$  are QCD and electroweak penguin operators, and  $Q_{7\gamma}$  and  $Q_{8g}$  are the electromagnetic and chromomagnetic dipole operators. They are given by

$$\begin{aligned} Q_1^p &= (\bar{p}b)_{V-A}(\bar{s}p)_{V-A}, & Q_2^p &= (\bar{p}_i b_j)_{V-A}(\bar{s}_j p_i)_{V-A}, \\ Q_3 &= (\bar{s}b)_{V-A} \sum_q (\bar{q}q)_{V-A}, & Q_4 &= (\bar{s}_i b_j)_{V-A} \sum_q (\bar{q}_j q_i)_{V-A}, \\ Q_5 &= (\bar{s}b)_{V-A} \sum_q (\bar{q}q)_{V+A}, & Q_6 &= (\bar{s}_i b_j)_{V-A} \sum_q (\bar{q}_j q_i)_{V+A}, \\ Q_7 &= (\bar{s}b)_{V-A} \sum_q \frac{3}{2} e_q (\bar{q}q)_{V+A}, & Q_8 &= (\bar{s}_i b_j)_{V-A} \sum_q \frac{3}{2} e_q (\bar{q}_j q_i)_{V+A}, \\ Q_9 &= (\bar{s}b)_{V-A} \sum_q \frac{3}{2} e_q (\bar{q}q)_{V-A}, & Q_{10} &= (\bar{s}_i b_j)_{V-A} \sum_q \frac{3}{2} e_q (\bar{q}_j q_i)_{V-A}, \\ Q_{7\gamma} &= \frac{-e}{8\pi^2} m_b \bar{s}\sigma_{\mu\nu} (1 + \gamma_5) F^{\mu\nu} b, & Q_{8g} &= \frac{-g_s}{8\pi^2} m_b \bar{s}\sigma_{\mu\nu} (1 + \gamma_5) G^{\mu\nu} b, \end{aligned} \quad (2)$$

where  $(\bar{q}_1 q_2)_{V\pm A} = \bar{q}_1 \gamma_\mu (1 \pm \gamma_5) q_2$ ,  $i, j$  are colour indices,  $e_q$  are the electric charges of the quarks in units of  $|e|$ , and a summation over  $q = u, d, s, c, b$  is implied. The definition of the dipole operators  $Q_{7\gamma}$  and  $Q_{8g}$  corresponds to the sign convention  $iD^\mu = i\partial^\mu + g_s A_a^\mu t_a$  for the gauge-covariant derivative. The Wilson coefficients are calculated at a high scale  $\mu \sim M_W$  and evolved down to a characteristic scale  $\mu \sim m_b$  using next-to-leading order renormalization-group equations. The essential problem obstructing the calculation of non-leptonic decay amplitudes resides in the evaluation of the hadronic matrix elements of the local operators contained in the effective Hamiltonian.

NLO	$C_1$	$C_2$	$C_3$	$C_4$	$C_5$	$C_6$
$\mu = m_b/2$	1.137	-0.295	0.021	-0.051	0.010	-0.065
$\mu = m_b$	1.081	-0.190	0.014	-0.036	0.009	-0.042
$\mu = 2m_b$	1.045	-0.113	0.009	-0.025	0.007	-0.027
	$C_7/\alpha$	$C_8/\alpha$	$C_9/\alpha$	$C_{10}/\alpha$	$C_{7\gamma}^{\text{eff}}$	$C_{8g}^{\text{eff}}$
$\mu = m_b/2$	-0.024	0.096	-1.325	0.331	—	—
$\mu = m_b$	-0.011	0.060	-1.254	0.223	—	—
$\mu = 2m_b$	0.011	0.039	-1.195	0.144	—	—
LO	$C_1$	$C_2$	$C_3$	$C_4$	$C_5$	$C_6$
$\mu = m_b/2$	1.185	-0.387	0.018	-0.038	0.010	-0.053
$\mu = m_b$	1.117	-0.268	0.012	-0.027	0.008	-0.034
$\mu = 2m_b$	1.074	-0.181	0.008	-0.019	0.006	-0.022
	$C_7/\alpha$	$C_8/\alpha$	$C_9/\alpha$	$C_{10}/\alpha$	$C_{7\gamma}^{\text{eff}}$	$C_{8g}^{\text{eff}}$
$\mu = m_b/2$	-0.012	0.045	-1.358	0.418	-0.364	-0.169
$\mu = m_b$	-0.001	0.029	-1.276	0.288	-0.318	-0.151
$\mu = 2m_b$	0.018	0.019	-1.212	0.193	-0.281	-0.136

TABLE I. Wilson coefficients  $C_i$  in the NDR scheme. Input parameters are  $\Lambda_{\overline{\text{MS}}}^{(5)} = 0.225 \text{ GeV}$ ,  $m_t(m_t) = 167 \text{ GeV}$ ,  $m_b(m_b) = 4.2 \text{ GeV}$ ,  $M_W = 80.4 \text{ GeV}$ ,  $\alpha = 1/129$ , and  $\sin^2 \theta_W = 0.23$  [23].

### III. QCD FACTORIZATION IN $B \rightarrow PV$ DECAYS

When the QCD factorization (QCDF) method is applied to the decays  $B \rightarrow PV$ , the hadronic matrix elements of the local effective operators can be written as

$$\begin{aligned} \langle PV | \mathcal{O}_i | B \rangle = & F_1^{B \rightarrow P}(0) T_{V,i}^I \star f_V \Phi_V + A_0^{B \rightarrow V}(0) T_{P,i}^I \star f_P \Phi_P \\ & + T_i^{II} \star f_B \Phi_B \star f_V \Phi_V \star f_P \Phi_P, \end{aligned} \quad (3)$$

where  $\Phi_M$  are leading-twist light-cone distribution amplitudes, and the  $\star$ -products imply an integration over the light-cone momentum fractions of the constituent quarks inside the mesons. A graphical representation of this result is shown in Figure 1.

Here  $F_1^{B \rightarrow P}$  and  $A_0^{B \rightarrow V}$  denote the form factors for  $B \rightarrow P$  and  $B \rightarrow V$  transitions, respectively.  $\Phi_B(\xi)$ ,  $\Phi_V(x)$ , and  $\Phi_P(y)$  are the light-cone distribution amplitudes (LCDA) of valence quark Fock states for  $B$ , vector, and pseudoscalar mesons, respectively.  $T_i^{I,II}$  denote the hard-scattering kernels, which are dominated by hard gluon exchange when the power suppressed  $\mathcal{O}(\Lambda_{QCD}/m_b)$  terms are neglected. So they are calculable order by order in perturbation theory. The leading terms of  $T^I$  come from the tree level and correspond to the naive factorization (NF) approximation. The order of  $\alpha_s$  terms of  $T^I$  can be depicted by vertex-correction diagrams Fig.2 (a-d) and penguin-correction diagrams Fig.2 (e-f).  $T^{II}$  describes the hard interactions between the spectator quark and the emitted meson  $M_2$  when the gluon virtuality is large. Its lowest order terms are  $\mathcal{O}(\alpha_s)$  and can be depicted by hard spectator scattering diagrams Fig.2 (g-h). One of the most interesting results of the QCDF approach is that, in the heavy quark limit, the strong phases arise naturally from the hard-scattering kernels at the order of  $\alpha_s$ . As for the nonperturbative part, they are, as already mentioned, taken into account by the form factors and the LCDA of mesons up to corrections which are power suppressed in  $1/m_b$ .

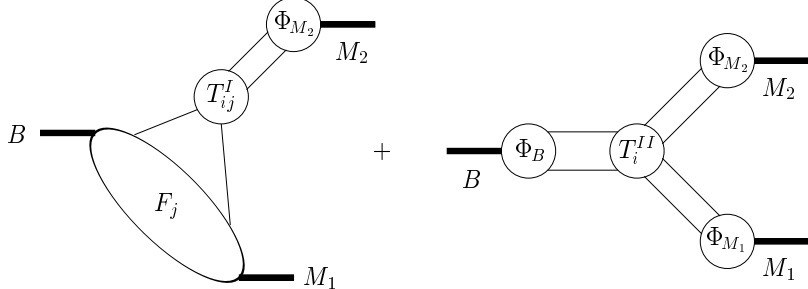


FIG. 1. Graphical representation of the factorization formula. Only one of the two form-factor terms in (3) is shown for simplicity.

With the above discussions on the effective Hamiltonian of  $B$  decays Eq.(1) and the QCDF expressions of hadronic matrix elements Eq.(3), the decay amplitudes for  $B \rightarrow P V$  in the heavy quark limit can be written as

$$\mathcal{A}(B \rightarrow PV) = \frac{G_F}{\sqrt{2}} \sum_{p=u,c} \sum_{i=1}^{10} \lambda_p a_i^p \langle PV | \mathcal{O}_i | B \rangle_{nf}. \quad (4)$$

The above  $\langle PV | \mathcal{O}_i | B \rangle_{nf}$  are the factorized hadronic matrix elements, which have the same definitions as those in the NF approach. The “nonfactorizable” effects are included in the coefficients  $a_i$  which are process dependent. The coefficients  $a_i$  are collected in Sec. III A, and the explicit expressions for the decay amplitudes of  $B \rightarrow P V$  can be found in the appendix A.

According to the arguments in [22], the contributions of weak annihilation to the decay amplitudes are power suppressed, and they do not appear in the QCDF formula Eq.(3). But, as emphasized in [40,42,43], the contributions from weak annihilation could give large strong phases with QCD corrections, and hence large CP violation could be expected, so their effects cannot simply be neglected. However, in the QCDF method, the annihilation topologies (see Fig.3) violate factorization because of the endpoint divergence. There is similar endpoint divergence when considering the chirally enhanced hard spectator scattering. One possible way is to treat the endpoint divergence from different sources as different phenomenological parameters [23]. The corresponding price is the introduction of model dependence and extra numerical uncertainties in the decay amplitudes. In this work, we will follow the treatment of Ref. [23] and express the weak annihilation topological decay amplitudes as

$$\mathcal{A}^a(B \rightarrow PV) \propto f_B f_P f_V \sum \lambda_p b_i, \quad (5)$$

where the parameters  $b_i$  are collected in Sec. III B, and the expressions for the weak annihilation decay amplitudes of  $B \rightarrow P V$  are listed in the appendix B.

### A. The QCD coefficients $a_i$

We express the QCD coefficients  $a_i$  (see Eq.(4) ) in two parts, i.e.,  $a_i = a_{i,I} + a_{i,II}$ . The first term  $a_{i,I}$  contains the naive factorisation and the vertex corrections which are described by Fig.2 (a-f), while the second part  $a_{i,II}$  corresponds to the hard spectator scattering diagrams Fig.2 (g-h).

There are two different cases according to the final states. Case I is that the recoiled meson  $M_1$  is a vector meson, and the emitted meson  $M_2$  corresponds to a pseudoscalar meson, and vice versa for case II. For case I, we sum up the results for  $a_i$  as follows:

$$\begin{aligned}
a_{1,I} &= C_1 + \frac{C_2}{N_c} \left[ 1 + \frac{C_F \alpha_s}{4\pi} V_M \right], & a_{1,II} &= \frac{\pi C_F \alpha_s}{N_c^2} C_2 H(BM_1, M_2), \\
a_{2,I} &= C_2 + \frac{C_1}{N_c} \left[ 1 + \frac{C_F \alpha_s}{4\pi} V_M \right], & a_{2,II} &= \frac{\pi C_F \alpha_s}{N_c^2} C_1 H(BM_1, M_2), \\
a_{3,I} &= C_3 + \frac{C_4}{N_c} \left[ 1 + \frac{C_F \alpha_s}{4\pi} V_M \right], & a_{3,II} &= \frac{\pi C_F \alpha_s}{N_c^2} C_4 H(BM_1, M_2), \\
a_{4,I}^p &= C_4 + \frac{C_3}{N_c} \left[ 1 + \frac{C_F \alpha_s}{4\pi} V_M \right] + \frac{C_F \alpha_s}{4\pi} \frac{P_{M,2}^p}{N_c}, & a_{4,II} &= \frac{\pi C_F \alpha_s}{N_c^2} C_3 H(BM_1, M_2), \\
a_{5,I} &= C_5 + \frac{C_6}{N_c} \left[ 1 - \frac{C_F \alpha_s}{4\pi} V'_M \right], & a_{5,II} &= -\frac{\pi C_F \alpha_s}{N_c^2} C_6 H'(BM_1, M_2), \\
a_{6,I}^p &= C_6 + \frac{C_5}{N_c} \left[ 1 - 6 \frac{C_F \alpha_s}{4\pi} \right] + \frac{C_F \alpha_s}{4\pi} \frac{P_{M,3}^p}{N_c}, & a_{6,II} &= 0, \\
a_{7,I} &= C_7 + \frac{C_8}{N_c} \left[ 1 - \frac{C_F \alpha_s}{4\pi} V'_M \right], & a_{7,II} &= -\frac{\pi C_F \alpha_s}{N_c^2} C_8 H'(BM_1, M_2), \\
a_{8,I}^p &= C_8 + \frac{C_7}{N_c} \left[ 1 - 6 \frac{C_F \alpha_s}{4\pi} \right] + \frac{\alpha}{9\pi} \frac{P_{M,3}^{p,ew}}{N_c}, & a_{8,II} &= 0, \\
a_{9,I} &= C_9 + \frac{C_{10}}{N_c} \left[ 1 + \frac{C_F \alpha_s}{4\pi} V_M \right], & a_{9,II} &= \frac{\pi C_F \alpha_s}{N_c^2} C_{10} H(BM_1, M_2), \\
a_{10,I}^p &= C_{10} + \frac{C_9}{N_c} \left[ 1 + \frac{C_F \alpha_s}{4\pi} V_M \right] + \frac{\alpha}{9\pi} \frac{P_{M,2}^{p,ew}}{N_c}, & a_{10,II} &= \frac{\pi C_F \alpha_s}{N_c^2} C_9 H(BM_1, M_2), 
\end{aligned} \tag{6}$$

where  $C_F = \frac{N_c^2 - 1}{2N_c}$ , and  $N_c = 3$ . The vertex parameters  $V_M$  and  $V'_M$  result from Fig.2 (a-d); the QCD penguin parameters  $P_{M,i}^p$  and the electroweak penguin parameters  $P_{M,i}^{p,ew}$  result from Fig.2 (e-f).

The vertex corrections are given by:

$$\begin{aligned}
V_M &= 12 \ln \frac{m_b}{\mu} - 18 + \int_0^1 dx g(x) \Phi_M(x), \\
V'_M &= 12 \ln \frac{m_b}{\mu} - 6 + \int_0^1 dx g(1-x) \Phi_M(x), \\
g(x) &= 3 \left( \frac{1-2x}{1-x} \ln x - i\pi \right) \\
&\quad + \left[ 2 \text{Li}_2(x) - \ln^2 x + \frac{2 \ln x}{1-x} - (3 + 2i\pi) \ln x - (x \leftrightarrow 1-x) \right], 
\end{aligned} \tag{7}$$

where  $\text{Li}_2(x)$  is the dilogarithm function, whereas the constants 18 and 6 are specific to the NDR scheme.

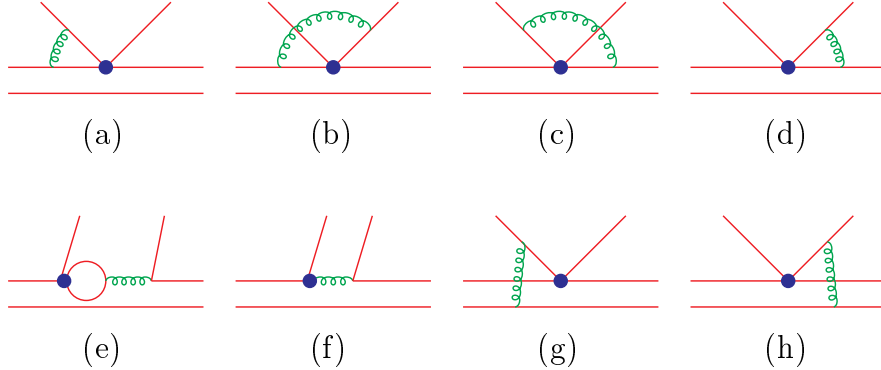


FIG. 2. Order  $\alpha_s$  corrections to the hard-scattering kernels. The upward quark lines represent the emitted mesons from b quark weak decays. These diagrams are commonly called vertex corrections, penguin corrections, and hard spectator scattering diagrams for Fig. (a-d), Fig. (e-f), and Fig. (g-h) respectively.

The penguin contributions are:

$$\begin{aligned}
P_{M,2}^p &= C_1 \left[ \frac{4}{3} \ln \frac{m_b}{\mu} + \frac{2}{3} - G_M(s_p) \right] + \left( C_3 - \frac{1}{2} C_9 \right) \left[ \frac{8}{3} \ln \frac{m_b}{\mu} + \frac{4}{3} - G_M(0) - G_M(1) \right] \\
&\quad + \sum_{q=q'} \left( C_4 + C_6 + \frac{3}{2} e_q C_8 + \frac{3}{2} e_q C_{10} \right) \left[ \frac{4}{3} \ln \frac{m_b}{\mu} - G_M(s_q) \right] - 2 C_{8g}^{\text{eff}} \int_0^1 dx \frac{\Phi_M(x)}{1-x}, \\
P_{M,3}^p &= C_1 \left[ \frac{4}{3} \ln \frac{m_b}{\mu} + \frac{2}{3} - \hat{G}_M(s_p) \right] + \left( C_3 - \frac{1}{2} C_9 \right) \left[ \frac{8}{3} \ln \frac{m_b}{\mu} + \frac{4}{3} - \hat{G}_M(0) - \hat{G}_M(1) \right] \\
&\quad + \sum_{q=q'} \left( C_4 + C_6 + \frac{3}{2} e_q C_8 + \frac{3}{2} e_q C_{10} \right) \left[ \frac{4}{3} \ln \frac{m_b}{\mu} - \hat{G}_M(s_q) \right] - 2 C_{8g}^{\text{eff}}, \tag{8}
\end{aligned}$$

and the electroweak penguin parameters  $P_{M,i}^{p,ew}$ :

$$\begin{aligned}
P_{M,2}^{p,ew} &= \left( C_1 + N_c C_2 \right) \left[ \frac{4}{3} \ln \frac{m_b}{\mu} + \frac{2}{3} - G_M(s_p) \right] - \left( C_3 + N_c C_4 \right) \left[ \frac{4}{3} \ln \frac{m_b}{\mu} + \frac{2}{3} - \frac{1}{2} G_M(0) - \frac{1}{2} G_M(1) \right] \\
&\quad + \sum_{q=q'} \left( N_c C_3 + C_4 + N_c C_5 + C_6 \right) \frac{3}{2} e_q \left[ \frac{4}{3} \ln \frac{m_b}{\mu} - G_M(s_q) \right] - N_c C_{7\gamma}^{\text{eff}} \int_0^1 dx \frac{\Phi_M(x)}{1-x}, \\
P_{M,3}^{p,ew} &= \left( C_1 + N_c C_2 \right) \left[ \frac{4}{3} \ln \frac{m_b}{\mu} + \frac{2}{3} - \hat{G}_M(s_p) \right] - \left( C_3 + N_c C_4 \right) \left[ \frac{4}{3} \ln \frac{m_b}{\mu} + \frac{2}{3} - \frac{1}{2} \hat{G}_M(0) - \frac{1}{2} \hat{G}_M(1) \right] \\
&\quad + \sum_{q=q'} \left( N_c C_3 + C_4 + N_c C_5 + C_6 \right) \frac{3}{2} e_q \left[ \frac{4}{3} \ln \frac{m_b}{\mu} - \hat{G}_M(s_q) \right] - N_c C_{7\gamma}^{\text{eff}}, \tag{9}
\end{aligned}$$

where  $s_q = m_q^2/m_b^2$ , and where  $q'$  in the expressions for  $P_{M,i}^p$  and  $P_{M,i}^{p,ew}$  runs over all the active quarks at the scale  $\mu = \mathcal{O}(m_b)$ , i.e.,  $q' = u, d, s, c, b$ . The functions  $G_M(s)$  and  $\hat{G}_M(s)$  are given respectively by:

$$G_M(s) = \int_0^1 dx G(s - i\epsilon, 1-x) \Phi_M(x), \tag{10}$$

$$\hat{G}_M(s) = \int_0^1 dx G(s - i\epsilon, 1-x) \Phi_M^p(x), \tag{11}$$

$$\begin{aligned}
G(s, x) &= -4 \int_0^1 du u(1-u) \ln[s - u(1-u)x] \\
&= \frac{2(12s + 5x - 3x \ln s)}{9x} - \frac{4\sqrt{4s-x}(2s+x)}{3x^{3/2}} \arctan \sqrt{\frac{x}{4s-x}}. \tag{12}
\end{aligned}$$

The parameters  $H(BM_1, M_2)$  and  $H'(BM_1, M_2)$  in  $a_{i,II}$ , which originate from hard gluon exchanges between the spectator quark and the emitted meson  $M_2$ , are written as:

$$\begin{aligned}
H(BV, P) &= \frac{f_B f_V}{m_B^2 A_0^{B \rightarrow V}(0)} \int_0^1 d\xi \int_0^1 dx \int_0^1 dy \frac{\Phi_B(\xi)}{\xi} \frac{\Phi_P(x)}{\bar{x}} \frac{\Phi_V(y)}{\bar{y}}, \\
H'(BV, P) &= \frac{f_B f_V}{m_B^2 A_0^{B \rightarrow V}(0)} \int_0^1 d\xi \int_0^1 dx \int_0^1 dy \frac{\Phi_B(\xi)}{\xi} \frac{\Phi_P(x)}{x} \frac{\Phi_V(y)}{\bar{y}}.
\end{aligned} \tag{13}$$

For case II (vector meson emitted) except for the parameters of  $H(BM_1, M_2)$  and  $H'(BM_1, M_2)$ , the expressions for  $a_i$  are similar to those in case I. However we would like to point out that, because  $\langle V | (\bar{q}q)_{S \pm P} | 0 \rangle = 0$ , the contributions of the effective operators  $\mathcal{O}_{6,8}$  to the hadronic matrix elements vanish, i.e., the terms that are related to  $a_{6,8}$  disappear from the decay amplitudes for case II. As to the parameters  $H(BM_1, M_2)$  and  $H'(BM_1, M_2)$  in  $a_{i,II}$ , they are defined as

$$\begin{aligned}
H(BP, V) &= \frac{f_B f_P}{m_B^2 F_1^{B \rightarrow P}(0)} \int_0^1 d\xi \int_0^1 dx \int_0^1 dy \frac{\Phi_B(\xi)}{\xi} \frac{\Phi_V(x)}{\bar{x}} \left[ \frac{\Phi_P(y)}{\bar{y}} + \frac{2\mu_P}{m_b} \frac{\bar{x}}{x} \frac{\Phi_P^p(y)}{\bar{y}} \right], \\
H'(BP, V) &= -\frac{f_B f_P}{m_B^2 F_1^{B \rightarrow P}(0)} \int_0^1 d\xi \int_0^1 dx \int_0^1 dy \frac{\Phi_B(\xi)}{\xi} \frac{\Phi_V(x)}{x} \left[ \frac{\Phi_P(y)}{\bar{y}} + \frac{2\mu_P}{m_b} \frac{x}{\bar{x}} \frac{\Phi_P^p(y)}{\bar{y}} \right].
\end{aligned} \tag{14}$$

The parameter  $\mu_P = m_P^2 / (m_1 + m_2)$  where  $m_{1,2}$  are the current quark masses of the meson constituents, is proportional the the chiral quark condensate.

## B. The annihilation parameters $b_i$

The parameters of  $b_i$  in Eq.(5) correspond to weak annihilation contributions. Now we give their expressions, which are analogous to those in [23]:

$$\begin{aligned}
b_1(M_1, M_2) &= \frac{C_F}{N_c^2} C_1 A_1^i(M_1, M_2), \\
b_2(M_1, M_2) &= \frac{C_F}{N_c^2} C_2 A_1^i(M_1, M_2), \\
b_3(M_1, M_2) &= \frac{C_F}{N_c^2} \left\{ C_3 A_1^i(M_1, M_2) + C_5 A_3^i(M_1, M_2) + [C_5 + N_c C_6] A_3^f(M_1, M_2) \right\}, \\
b_4(M_1, M_2) &= \frac{C_F}{N_c^2} \left\{ C_4 A_1^i(M_1, M_2) + C_6 A_2^i(M_1, M_2) \right\}, \\
b_3^{ew}(M_1, M_2) &= \frac{C_F}{N_c^2} \left\{ C_9 A_1^i(M_1, M_2) + C_7 A_3^i(M_1, M_2) + [C_7 + N_c C_8] A_3^f(M_1, M_2) \right\}, \\
b_4^{ew}(M_1, M_2) &= \frac{C_F}{N_c^2} \left\{ C_{10} A_1^i(M_1, M_2) + C_8 A_2^i(M_1, M_2) \right\}.
\end{aligned} \tag{15}$$

Here the current-current annihilation parameters  $b_{1,2}(M_1, M_2)$  arise from the hadronic matrix elements of the effective operators  $\mathcal{O}_{1,2}$ , the QCD penguin annihilation parameters  $b_{3,4}(M_1, M_2)$  from  $\mathcal{O}_{3-6}$ , and the electroweak penguin annihilation parameters  $b_{3,4}^{ew}(M_1, M_2)$  from  $\mathcal{O}_{7-10}$ . The parameters of  $b_i$  are closely related to the final states; they can also be divided into two different cases according to the final states. Case I is that  $M_1$  is a vector meson, and  $M_2$  is a pseudoscalar meson (here  $M_1$  and  $M_2$  are tagged in Fig. 3). Case II is that  $M_1$  corresponds to a pseudoscalar meson, and  $M_2$  corresponds to a vector meson. For case I, the definitions of  $A_k^{i,f}(M_1, M_2)$  in Eq.(15) are

$$\begin{aligned}
A_{1,2}^f(V, P) &= 0, \\
A_3^f(V, P) &= \pi \alpha_s \int_0^1 dx \int_0^1 dy \Phi_V(x) \Phi_P^p(y) \frac{2\mu_P}{m_b} \frac{2(1+\bar{x})}{\bar{x}^2 y}, \\
A_1^i(V, P) &= \pi \alpha_s \int_0^1 dx \int_0^1 dy \Phi_V(x) \Phi_P(y) \left[ \frac{1}{y(1-x\bar{y})} + \frac{1}{\bar{x}^2 y} \right], \\
A_2^i(V, P) &= -\pi \alpha_s \int_0^1 dx \int_0^1 dy \Phi_V(x) \Phi_P(y) \left[ \frac{1}{\bar{x}(1-x\bar{y})} + \frac{1}{\bar{x} y^2} \right], \\
A_3^i(V, P) &= \pi \alpha_s \int_0^1 dx \int_0^1 dy \Phi_V(x) \Phi_P^p(y) \frac{2\mu_P}{m_b} \frac{2\bar{y}}{\bar{x} y(1-x\bar{y})}.
\end{aligned} \tag{16}$$

For case-II,

$$\begin{aligned}
A_{1,2}^f(P, V) &= 0, \\
A_3^f(P, V) &= -\pi\alpha_s \int_0^1 dx \int_0^1 dy \Phi_P^p(x) \Phi_V(y) \frac{2\mu_P}{m_b} \frac{2(1+y)}{\bar{x}y^2}, \\
A_1^i(P, V) &= \pi\alpha_s \int_0^1 dx \int_0^1 dy \Phi_P(x) \Phi_V(y) \left[ \frac{1}{y(1-x\bar{y})} + \frac{1}{\bar{x}^2 y} \right], \\
A_2^i(P, V) &= -\pi\alpha_s \int_0^1 dx \int_0^1 dy \Phi_P(x) \Phi_V(y) \left[ \frac{1}{\bar{x}(1-x\bar{y})} + \frac{1}{\bar{x}y^2} \right], \\
A_3^i(P, V) &= \pi\alpha_s \int_0^1 dx \int_0^1 dy \Phi_P^p(x) \Phi_V(y) \frac{2\mu_P}{m_b} \frac{2x}{\bar{x}y(1-x\bar{y})}. \tag{17}
\end{aligned}$$

Here our notation and convention are the same as those in [23]. The superscripts  $i$  and  $f$  on  $A^{i,f}$  correspond to the contributions from Fig. 3(a-b) and Fig. 3(c-d), respectively. The subscripts  $k = 1, 2, 3$  on  $A_k^{i,f}$  refer to the Dirac structures  $(V - A) \otimes (V - A)$ ,  $(V - A) \otimes (V + A)$  and  $(-2)(S - P) \otimes (S + P)$ , respectively.  $\Phi_V(x)$  denotes the leading-twist LCDAs of a vector meson, and  $\Phi_P(x)$  and  $\Phi_P^p(x)$  denote twist-2 and twist-3 LCDAs of a pseudoscalar meson, respectively.

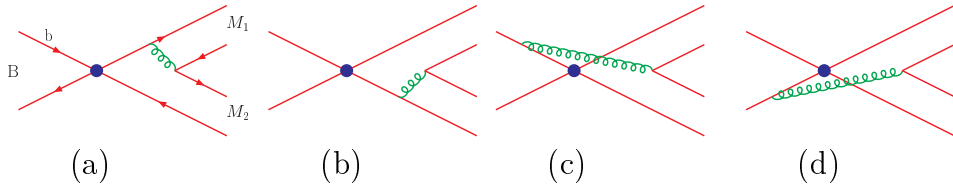


FIG. 3. Order  $\alpha_s$  corrections to the weak annihilations of charmless decays  $B \rightarrow PV$ .

Note that assuming  $SU(3)$  flavor symmetry implies symmetric LCDAs of light mesons (under  $x \leftrightarrow \bar{x}$ ), whence  $A_1^i = -A_2^i$ . In this approximation the weak annihilation contributions (for case I) can be parametrized as

$$\begin{aligned}
A_1^i(V, P) &\simeq 18\pi\alpha_s \left( X_A - 4 + \frac{\pi^2}{3} \right), \\
A_3^i(V, P) &\simeq \pi\alpha_s r_\chi \left[ 2\pi^2 - 6 \left( X_A^2 + 2X_A \right) \right], \\
A_3^f(V, P) &\simeq 6\pi\alpha_s r_\chi \left( 2X_A^2 - X_A \right), \tag{18}
\end{aligned}$$

where  $X_A = \int_0^1 dx/x$  parametrizes the divergent endpoint integrals and  $r_\chi = 2\mu_P/m_b$  is the so-called *chirally enhanced* factor. We can get similar forms to Eq.(18) for case II, but with  $A_3^f(P, V) = -A_3^f(V, P)$ . In our calculation, we will treat  $X_A$  as a phenomenological parameter, and take the same value for all annihilation terms, although this approximation is crude and there is no known physical argument justifying this assumption. We shall see below that  $X_A$  gives large uncertainties in the theoretical prediction.

#### IV. QCD FACTORISATION VERSUS EXPERIMENT

In order to propose a test of QCD factorization with respect to experiment, a compilation of various charmless branching fractions and direct  $CP$  asymmetries was performed and is given in tables II, III and IV. This compilation includes the latest results from BaBar, Belle and CLEO. The measurements were combined into a single central value and error, that may be compared with the theoretical prediction. First, the total error from each experiment was computed by summing quadratically the statistic and systematic error: this approach is valid in the limit that the systematic error is not so large with respect to the statistic error. Secondly, when the experiment provides an asymmetric error  $^{+\sigma_1}_{-\sigma_2}$ , a conservative symmetric error was assumed in the calculation by using  $\pm \text{Max}(\sigma_1, \sigma_2)$ . In case of a disagreement between several experiments for a given measurement, the

total error was increased by a “scale factor” computed from a  $\chi^2$  combining the various experiments, using the standard procedure given by the PDG [44].

In order to compare the theoretical predictions  $\{y\}$  with the experimental measurements  $\{x \pm \sigma_x\}$ , the following  $\chi^2$  was defined:

$$\chi^2 = \sum \left( \frac{x - y}{\sigma_x} \right)^2.$$

In the case when a correlation matrix between several measurements is given by the experiment, as in the case of the  $\rho^+ \pi^- / \rho^+ K^-$  measurements, the  $\chi^2$  was corrected to account for it. The above  $\chi^2$  was then minimized using MINUIT [46], letting free all theoretical parameters in their allowed range. The quality of the minimum yielded by MINUIT was assessed by replacing it with an ad hoc minimizer scanning the entire parameter space. The theoretical predictions, with the theoretical parameters yielding the best fits, are compared to experiment in table VI for two scenarios to be explained below. The asymmetries of the  $\rho^\pm \pi^\mp$  channels can be expressed [9] in terms of the quantities reported in table IV. The comparison between their theoretical predictions and experiment is reported in table VII.

Scenario 1 refers to a fit according to QCD factorisation, varying all theoretical parameters in the range presented in table V. Even the unitarity triangle angle  $\gamma$  is varied freely and ends up not far from 90 degrees. We have taken  $X_A = X_H$  in the range proposed in ref. [23]:

$$X_{A,H} = \int_0^1 \frac{dx}{x} = \ln \frac{m_B}{\Lambda_h} (1 + \rho_{A,H} e^{i\phi_{A,H}}). \quad (19)$$

These parameters label our ignorance of the non perturbatively calculable subdominant contribution to the annihilation and hard scattering, defined in Eqs. (16, 17) and Eqs. (13, 14) respectively. They do not need to have the same value for all  $PV$  channels but we have nevertheless assumed one common value since a fit would become impossible with too many unknown parameters.

Scenario 2 in table VI refers to a fit adding a charming penguin inspired long distance contribution which will be presented and discussed in section V. In this fit  $\gamma$  is constrained within the range  $[34^\circ, 82^\circ]$ .

The values of the theoretical parameters found for the two best fits is given in table V: many parameters are found to be at the edge of their allowed range<sup>††</sup>. In order to estimate the quality of the agreement between measurements and predictions, the standard Monte Carlo based “goodness of fit” test was performed:

- the best-fit values of the theoretical parameters were used to make predictions for the branching ratios and  $CP$  asymmetries,
- the total experimental error from each measurement was used to generate new experimental values distributed around the predictions with a Gaussian probability,
- the full fit previously performed on real measurements is now run on this simulated data, and the  $\chi^2$  of this fit is saved in a histogram  $H$ .

It is then possible to compare the  $\chi^2_{\text{data}}$  obtained from the measurement with the  $\chi^2$  one would obtain if the predictions were true. Additionally, one may compute the confidence level of the tested model by using:

$$CL \leq \frac{\int_{\chi^2 > \chi^2_{\text{data}}} H(\chi^2) d\chi^2}{\int_{\chi^2 > 0} H(\chi^2) d\chi^2}.$$

The results of the “goodness of fit” tests are given in FIG. IV. From these tests, one may quote an upper limit for the confidence level in scenario 1,  $CL \leq 0.1\%$ , and in the case of scenario 2,  $CL \leq 7.7\%$ .

---

<sup>††</sup>Table 5 shows that the fit value of  $\rho_A$  appears at the edge of the input range,  $\rho_A = 1$ . However enlarging the range of  $\rho_A$ , such as  $|\rho_A| \leq 10$ , brings a large annihilation contributions  $(\rho_A, \phi_A) = (2.3, -41^\circ)$  for scenario 1 and  $(4.4, -108^\circ)$  for scenario 2. With so large values of  $|\rho_A|$  the unpredictable contributions would dominate the total result making the whole exercise void of signification.

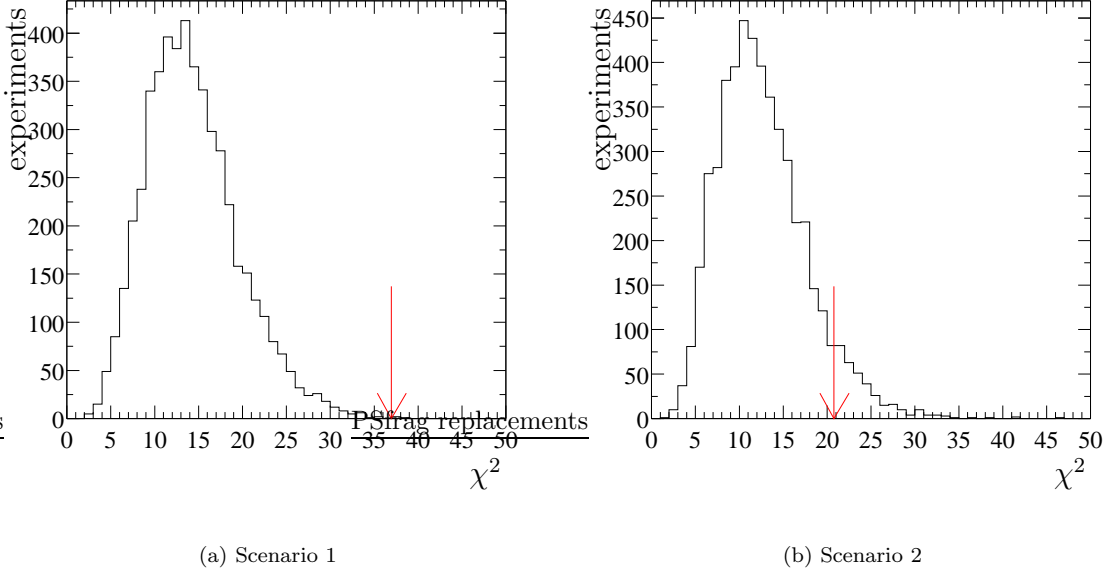


FIG. 4. Goodness of fit test of the two proposed theoretical models: the arrow points at the value  $\chi^2_{\text{data}}$  found from the measurements, and the histogram shows the values allowed for  $\chi^2$  in the case that the models predictions are correct.

$\mathcal{BR}(\times 10^6)$	BaBar [1–10]	Belle [11–15]	CLEO [16–21]	Average
$B^0 \rightarrow \pi^\pm \rho^\mp$	$28.9 \pm 5.4 \pm 4.3$	$20.8^{+6.0+2.8}_{-6.3-3.1}$	$27.6^{+8.4}_{-7.4} \pm 4.2$	$25.53 \pm 4.32$
$B^+ \rightarrow \pi^+ \rho^0$	$24 \pm 8 \pm 3 (< 39)$	$8.0^{+2.3}_{-2.0} \pm 0.7$	$10.4^{+3.3}_{-3.4} \pm 2.1$	$9.49 \pm 2.57$
$B^0 \rightarrow \pi^0 \rho^0$	$3.6 \pm 3.5 \pm 1.7 (< 10.6)$	$< 5.3$	$1.6^{+2.0}_{-1.4} \pm 0.8 (< 5.5)$	$2.07 \pm 1.88$
$B^+ \rightarrow \pi^+ \omega$	$6.6^{+2.1}_{-1.8} \pm 0.7$	$4.2^{+2.0}_{-1.8} \pm 0.5$	$11.3^{+3.3}_{-2.9} \pm 1.4$	$6.22 \pm 1.70$
$B^0 \rightarrow K^+ \rho^-$	–	$15.8^{+5.1+1.7}_{-4.6-3.0}$	$16.0^{+7.6}_{-6.4} \pm 2.8 (< 32)$	$15.88 \pm 4.65$
$B^+ \rightarrow K^+ \rho^0$	$10 \pm 6 \pm 2 (< 29)$	–	$8.4^{+4.0}_{-3.4} \pm 1.8 (< 17)$	$8.92 \pm 3.60$
$B^+ \rightarrow K^+ \omega$	$1.4^{+1.3}_{-1.0} \pm 0.3 (< 4)$	$9.2^{+2.6}_{-2.3} \pm 1.0$	$3.2^{+2.4}_{-1.9} \pm 0.8 (< 7.9)$	$2.92 \pm 1.94$
$B^0 \rightarrow K^0 \omega$	$5.9^{+1.7}_{-1.5} \pm 0.9$	–	$10.0^{+5.4}_{-4.2} \pm 1.4 (< 21)$	$6.34 \pm 1.82$
$B^0 \rightarrow K^* + \pi^-$	–	$26.0 \pm 8.3 \pm 3.5$	$16^{+6}_{-5} \pm 2$	$19.3 \pm 5.2$
$B^+ \rightarrow K^{*0} \pi^-$	$15.5 \pm 3.4 \pm 1.8$	$19.4^{+4.2}_{-3.9} \pm 2.1^{+3.5}_{-6.8}$	$7.6^{+3.5}_{-3.0} \pm 1.6 (< 16)$	$12.12 \pm 3.13$
$B^+ \rightarrow K^{*+} \pi^0$	–	–	$7.1^{+11.4}_{-7.1} \pm 1.0 (< 31)$	$7.1 \pm 11.4$
$B^+ \rightarrow K^* + \eta$	$22.1^{+11.1}_{-9.2} \pm 3.3$	$26.5^{+7.8}_{-7.0} \pm 3.0$	$26.4^{+9.6}_{-8.2} \pm 3.3$	$25.4 \pm 5.6$
$B^0 \rightarrow K^{*0} \eta$	$19.8^{+6.5}_{-5.6} \pm 1.7$	$16.5^{+4.6}_{-4.2} \pm 1.2$	$13.8^{+5.5}_{-4.6} \pm 1.6$	$16.41 \pm 3.21$
$B^+ \rightarrow K^+ \phi$	$9.2 \pm 1.0 \pm 0.8$	$10.7 \pm 1.0^{+0.9}_{-1.6}$	$5.5^{+2.1}_{-1.8} \pm 0.6$	$8.58 \pm 1.24$
$B^0 \rightarrow K^0 \phi$	$8.7^{+1.7}_{-1.5} \pm 0.9$	$10.0^{+1.9+0.9}_{-1.7-1.3}$	$5.4^{+3.7}_{-2.7} \pm 0.7 (< 12.3)$	$8.72 \pm 1.37$

TABLE II. Experimentally known data of CP-averaged branching ratios for the charmless  $B \rightarrow PV$  decay modes, used as input for the global fit. The channels containing the  $\eta'$  meson have been excluded.

$\mathcal{A}_{CP}$	BaBar [1–10]	Belle [11–15]	CLEO [16–21]	Average
$B^- \rightarrow \pi^- \omega$	$-0.01^{+0.29}_{-0.31} \pm 0.03$	–	$-0.34 \pm 0.25 \pm 0.02$	$-0.21 \pm 0.19$
$B^- \rightarrow K^- \omega$	–	$-0.21 \pm 0.28 \pm 0.03$	–	$0.21 \pm 0.28$
$B^- \rightarrow K^* \eta$	–	$-0.05^{+0.25}_{-0.30} \pm 0.01$	–	$-0.05 \pm 0.30$
$\bar{B}^0 \rightarrow \bar{K}^* \eta$	–	$0.17^{+0.28}_{-0.25} \pm 0.01$	–	$0.17 \pm 0.28$
$B^- \rightarrow K^- \phi$	$-0.05 \pm 0.20 \pm 0.03$	–	–	$-0.05 \pm 0.20$

TABLE III. Experimental measured data of direct CP asymmetries for the charmless  $B \rightarrow PV$  decay modes, used as input for the global fit.

$B^0 \rightarrow \rho^\pm \pi^\mp$	Measurement	Correlation coefficient (%)			
		$\mathcal{A}_{CP}^{\rho\pi}$	$\mathcal{A}_{CP}^{\rho K}$	$\mathcal{C}_{\rho\pi}$	$\Delta\mathcal{C}_{\rho\pi}$
$\mathcal{A}_{CP}^{\rho\pi}$	$-0.22 \pm 0.08 \pm 0.07$	–	3.4	$-11.8$	$-10.4$
$\mathcal{A}_{CP}^{\rho K}$	$0.19 \pm 0.14 \pm 0.11$	3.4	–	$-1.3$	$-1.1$
$\mathcal{C}_{\rho\pi}$	$0.45^{+0.18}_{-0.19} \pm 0.09$	$-11.8$	$-1.3$	–	23.9
$\Delta\mathcal{C}_{\rho\pi}$	$0.38^{+0.19}_{-0.20} \pm 0.11$	$-10.4$	$-1.1$	23.9	–

TABLE IV. Experimental results and correlation matrix for the various asymmetries measured in the channels  $\rho^\pm \pi^\mp / \rho^\pm K^\mp$ . The notations are explained in [9].

In tables II (III) we give the experimental CP-averaged branching ratios (direct CP asymmetries) which we have used in our fits. We have also used the quantities reported in table IV which are related to the branching ratios and CP asymmetries of the  $B \rightarrow \rho^\pm \pi^\mp$  channels.

Input	Range	Scenario 1	Scenario 2
$\gamma$ (deg)		99.955	81.933
$m_s$ (GeV)	[0.085, 0.135]	0.085	0.085
$\mu$ (GeV)	[2.1, 8.4]	3.355	5.971
$\rho_A$	[−1, 1]	1.000	1.000
$\phi_A$ (deg)	[−180, 180]	−22.928	−87.907
$\lambda_B$ (GeV)	[0.2, 0.5]	0.500	0.500
$f_B$ (GeV)	[0.14, 0.22]	0.220	0.203
$R_u$	[0.35, 0.49]	0.350	0.350
$R_c$	[0.018, 0.025]	0.018	0.018
$A_0^{B \rightarrow \rho}$	[0.3162, 0.4278]	0.373	0.377
$F_1^{B \rightarrow \pi}$	[0.23, 0.33]	0.330	0.301
$A_0^{B \rightarrow \omega}$	[0.25, 0.35]	0.350	0.326
$A_0^{B \rightarrow K^*}$	[0.3995, 0.5405]	0.400	0.469
$F_1^{B \rightarrow K}$	[0.28, 0.4]	0.333	0.280
$\text{Re}[\mathcal{A}^P]$	[−0.01, 0.01]		0.00253
$\text{Im}[\mathcal{A}^P]$	[−0.01, 0.01]		−0.00181
$\text{Re}[\mathcal{A}^V]$	[−0.01, 0.01]		−0.00187
$\text{Im}[\mathcal{A}^V]$	[−0.01, 0.01]		0.00049

TABLE V. Various theoretical inputs used in our global analysis of  $B \rightarrow PV$  decays in QCDF. The parameter ranges have been taken from literature [23], [34], [35] and [37]. The two last columns give the best fits of both scenarios.

	Experiment	Scenario 1		Scenario 2	
		Prediction	$\chi^2$	Prediction	$\chi^2$
$\mathcal{BR}(\bar{B}^0 \rightarrow \rho^0 \pi^0)$	$2.07 \pm 1.88$	0.132	1.1	0.177	1.0
$\mathcal{BR}(\bar{B}^0 \rightarrow \rho^+ \pi^-)$		11.023		10.962	
$\mathcal{BR}(\bar{B}^0 \rightarrow \rho^- \pi^+)$		18.374		17.429	
$\mathcal{BR}(\bar{B}^0 \rightarrow \rho^\pm \pi^\mp)$	$25.53 \pm 4.32$	29.397	0.8	28.391	0.4
$\mathcal{BR}(B^- \rightarrow \rho^0 \pi^-)$	$9.49 \pm 2.57$	9.889	0.0	7.879	0.4
$\mathcal{BR}(B^- \rightarrow \omega \pi^-)$	$6.22 \pm 1.7$	6.002	0.0	5.186	0.4
$\mathcal{BR}(B^- \rightarrow K^* \bar{K}^0)$		0.457		0.788	
$\mathcal{BR}(B^- \rightarrow K^{*0} K^-)$		0.490		0.494	
$\mathcal{BR}(B^- \rightarrow \Phi \pi^-)$		0.004		0.003	
$\mathcal{BR}(B^- \rightarrow \rho^- \pi^0)$		9.646		11.404	
$\mathcal{BR}(\bar{B}^0 \rightarrow \rho^0 \bar{K}^0)$		5.865		8.893	
$\mathcal{BR}(\bar{B}^0 \rightarrow \omega \bar{K}^0)$	$6.34 \pm 1.82$	2.318	4.9	5.606	0.2
$\mathcal{BR}(\bar{B}^0 \rightarrow \rho^+ K^-)$	$15.88 \pm 4.65$	6.531	4.0	14.304	0.1
$\mathcal{BR}(\bar{B}^0 \rightarrow K^{*-} \pi^+)$	$19.3 \pm 5.2$	9.760	3.4	10.787	2.7
$\mathcal{BR}(B^- \rightarrow K^{*-} \pi^0)$	$7.1 \pm 11.4$	7.303	0.0	8.292	0.0
$\mathcal{BR}(\bar{B}^0 \rightarrow \Phi \bar{K}^0)$	$8.72 \pm 1.37$	8.360	0.1	8.898	0.0
$\mathcal{BR}(B^- \rightarrow \bar{K}^{*0} \pi^-)$	$12.12 \pm 3.13$	7.889	1.8	11.080	0.1
$\mathcal{BR}(B^- \rightarrow \rho^0 K^-)$	$8.92 \pm 3.6$	1.882	3.8	5.655	0.8
$\mathcal{BR}(B^- \rightarrow \rho^- \bar{K}^0)$		7.140		14.006	
$\mathcal{BR}(B^- \rightarrow \omega K^-)$	$2.92 \pm 1.94$	2.398	0.1	6.320	3.1
$\mathcal{BR}(B^- \rightarrow \Phi K^-)$	$8.88 \pm 1.24$	8.941	0.0	9.479	0.2
$\mathcal{BR}(\bar{B}^0 \rightarrow \bar{K}^{*0} \eta)$	$16.41 \pm 3.21$	22.807	4.0	18.968	0.6
$\mathcal{BR}(B^- \rightarrow K^{*-} \eta)$	$25.4 \pm 5.6$	17.855	1.8	15.543	3.1
$\Delta \mathcal{C}_{\rho\pi}$	$0.38 \pm 0.23$	0.250		0.228	
$\mathcal{C}_{\rho\pi}$	$0.45 \pm 0.21$	0.019		0.092	
$\mathcal{A}_{CP}^{\rho\pi}$	$-0.22 \pm 0.11$	-0.015		-0.115	
$\mathcal{A}_{CP}^{\rho\kappa}$	$0.19 \pm 0.18$	0.060		0.197	
$\mathcal{A}_{CP}^{\omega\pi^-}$	$-0.21 \pm 0.19$	-0.072	0.5	-0.198	0.0
$\mathcal{A}_{CP}^{\omega\kappa^-}$	$-0.21 \pm 0.28$	0.029	0.7	0.189	2.0
$\mathcal{A}_{CP}^{\eta\kappa^{*-}}$	$-0.05 \pm 0.3$	-0.138	0.1	-0.217	0.3
$\mathcal{A}_{CP}^{\eta\bar{\kappa}^{*0}}$	$0.17 \pm 0.28$	-0.186	1.6	-0.158	1.4
$\mathcal{A}_{CP}^{\phi\kappa^-}$	$-0.05 \pm 0.2$	0.006	0.1	0.005	0.1
			36.9		20.8

TABLE VI. Best fit values using the global analysis of  $B \rightarrow PV$  decays in QCDF with free  $\gamma$  (scenario 1) and QCDF+Charming Penguins (scenario 2) with constrained  $\gamma$ . The CP-averaged branching ratios are in unit of  $10^{-6}$ .

	Experiment	Scenario 1	Scenario 2
$\mathcal{A}_{CP}^{\rho^+ \pi^-}$	$-0.82 \pm 0.31 \pm 0.16$	-0.04	-0.23
$\mathcal{A}_{CP}^{\rho^- \pi^+}$	$-0.11 \pm 0.16 \pm 0.09$	-0.0002	0.04

TABLE VII. Values of the CP asymmetries for  $B \rightarrow \pi\rho$  decays in QCDF (scenario 1) and QCDF+Charming Penguins (scenario 2). The notations are explained in [9].

For the sake of definiteness let us remind that the branching ratios for any charmless  $B$  decays,  $B \rightarrow PV$  channel, in the rest frame of the  $B$ -meson, is given by

$$\mathcal{BR}(B \rightarrow PV) = \frac{\tau_B}{8\pi m_B^2} \frac{|p|}{|p|} |\mathcal{A}(B \rightarrow PV) + \mathcal{A}^a(B \rightarrow PV) + \mathcal{A}^{\text{LD}}(B \rightarrow PV)|^2, \quad (20)$$

where  $\tau_B$  represents the  $B$ -meson life time (charged or uncharged according to the case). The amplitudes  $\mathcal{A}$ ,  $\mathcal{A}^a$  and  $\mathcal{A}^{\text{LD}}$  are defined in appendix A, B and in eqs. (24) and (25) respectively. In the case of pure QCD factorisation (scenario 1) we take of course  $\mathcal{A}^{\text{LD}} = 0$ . The kinematical factor  $|p|$  is written as:

$$|p| = \frac{\sqrt{[m_B^2 - (m_P + m_V)^2][m_B^2 - (m_P - m_V)^2]}}{2m_B}. \quad (21)$$

### A. Comparison with Du *et al*

Our negative conclusion about the QCD factorisation fit of the  $B \rightarrow PV$  channels is at odds with the conclusion of the authors of ref. [36], who have performed a successful fit of both  $B \rightarrow PP$  and  $B \rightarrow PV$  channels using the same theoretical starting point. These authors have excluded from their fits the channels containing a  $K^*$  in the final state, arguing that these channels seemed questionable to them. We have thus made a fit without the channels containing the  $K^*$ , and indeed we find as the authors of ref. [36] that the global agreement between QCD factorisation and experiment was satisfactory. Notice that this fit was done without discarding the channels  $B^+ \rightarrow \omega\pi^+(K^+)$  as done by Du *et al*.

Notice also that the parameters  $C_{\rho\pi}$  and the  $A_{CP}^{\rho\pi}$  have been kept in this fit. The disagreement between QCDF and experiment for these quantities was not enough to spoil the satisfactory agreement of the global fit because the experimental errors are still large on these quantities.

The conclusion of this subsection is that the difference between the “optimistic” conclusion about QCDF of Du *et al* and our rather pessimistic one comes from their choice of discarding the channels containing the  $K^*$ ’s. In other words the conclusion about the status of QCDF in the  $B \rightarrow PV$  channels depends on the confidence we give to the published results on these channels.

## V. A SIMPLE MODEL FOR LONG DISTANCE INTERACTIONS

As seen in table VI the failure of our overall fit with QCDF can be traced to two main facts. First the strange branching ratios are underestimated by QCDF. Second the direct CP asymmetries in the non-strange channels might also be underestimated. A priori this could be cured if some non-perturbative mechanism was contributing to  $|P|$ . Indeed, first, in the strange channels,  $|P|$  is Cabibbo enhanced and such a non-perturbative contribution could increase the branching ratios, and second, increasing  $|P|/|T|$  in the non-strange channels with non-small strong phases could increase significantly the direct CP asymmetries as already discussed. We have therefore tried a charming-penguin inspired model. We wanted nevertheless to avoid to add too many new parameters which would make the fit void of signification. We have therefore tried a model for long distance penguin contributions which depends only on two fitted complex numbers.

Let us start by describing our charming-penguin inspired model for strange final states. In the “charming penguin” picture the weak decay of a  $\bar{B}^0$  ( $B^-$ ) meson through the action of the operator  $Q_1^c$  (see notations in Eqs. (1) and (2)) creates an hadronic system containing the quarks  $s, \bar{d}(\bar{u}), c, \bar{c}$ , for example  $\bar{D}_s^{(*)} + D^{(*)}$  systems. This system goes to long distances, the  $c, \bar{c}$  eventually annihilate, a pair of light quarks are created by non-perturbative strong interaction and one is left with two light meson. Let us here restrict ourselves to the case of a  $PV$  pair of mesons, i.e. one of the final mesons is a light pseudoscalar ( $\pi, K, \eta$ ) and the other a light vector meson ( $\rho, \omega, \phi, K^*$ ). We leave aside from now on the  $\eta'$  which is presumably quite special.

We will picture now this hadronic system as a coherent state which decays into the two final mesons with total strangeness -1. This state has a total angular momentum  $J = 0$ . Its flavor  $s\bar{d}$  is that of a member of an octet of flavor- $SU(3)$ . We will assume flavor- $SU(3)$  symmetry in the decay amplitude of this hadronic state. This still leaves four  $SU(3)$ -invariant amplitudes since both  $P$  and  $V$  can have an octet and a singlet component and that there exist two octets in the decomposition of  $8 \times 8$ . We make a further simplifying assumption based on the OZI rule. Let us give an example: we assume that  $V = (s\bar{q})$  where  $q$  is any of the light quarks  $u, d, s$ , and that  $P = (q\bar{d})$ . Then we compute the contractions between

$$\langle (s\bar{q})(q\bar{d}) | s(\bar{u}u + \bar{d}d + \bar{s}s)\bar{d} \rangle = 1 \quad (22)$$

The meaning of this rule is simple. We add to the  $s\bar{d}$  quarks in our hadronic state an  $SU(3)$  singlet  $\bar{u}u + \bar{d}d + \bar{s}s$  and compute an “overlap” making contractions so that the quarks in the singlet go into two different mesons. This latter constraint is the OZI rule. This is why the overlap in Eq. (22) is 1 even if  $q = d$  since it is forbidden to have both  $d$  quarks from the singlet in the same final meson. As an example, the decay  $B \rightarrow \bar{K}^0 \rho^0$  gives the following overlap coefficient:

$$\langle (s\bar{d}) \frac{(u\bar{u} - d\bar{d})}{\sqrt{2}} | s(\bar{u}u + \bar{d}d + \bar{s}s)\bar{d} \rangle = -\frac{1}{\sqrt{2}} \quad (23)$$

For the  $\eta$  meson we will use the decomposition in [32]. The overlap coefficients thus computed play the role of  $SU(3)$  Clebsch-Gordan (CG) coefficients computed in a simple way. These coefficients are assumed to be multiplied by an universal complex amplitude to be fitted from experiment. Up to now we have assumed that the active quark (here  $s$ ) ended up in the vector meson. We need another universal amplitude for the case where the active quark ends up in the pseudoscalar meson.

We are thus left with two theoretically independent and unknown amplitudes, one with  $V = (s\bar{q})$ ,  $P = (q\bar{d})$ , one with  $P = (s\bar{q})$ ,  $V = (q\bar{d})$ . We shall write them respectively as  $\mathcal{A}^P$  ( $\mathcal{A}^V$ ) when the active quark ends up in the Pseudoscalar (Vector) meson.

Concerning the  $\bar{B}$  decay into a pseudoscalar + vector meson of vanishing total strangeness, we apply the same recipe with the same amplitudes  $\mathcal{A}^P$  and  $\mathcal{A}^V$ , replacing the  $s$  quark by a  $d$  quark and, of course, the corresponding replacement of the CKM factor  $V_{cb}V_{cs}^*$  by  $V_{cb}V_{cd}^*$ .

a. *To summarize* : the long distance term is given by two universal complex amplitudes multiplied by a CG coefficient computed simply by the overlap factor in (23), see table VIII.

	$Cl^P$	$Cl^V$
$\mathcal{BR}(\bar{B}^0 \rightarrow \rho^0 \pi^0)$	0.5	0.5
$\mathcal{BR}(\bar{B}^0 \rightarrow \rho^+ \pi^-)$	1.0	0.
$\mathcal{BR}(\bar{B}^0 \rightarrow \rho^- \pi^+)$	0.	1.0
$\mathcal{BR}(B^- \rightarrow \rho^0 \pi^-)$	$1/\sqrt{2}$	$-1/\sqrt{2}$
$\mathcal{BR}(B^- \rightarrow \omega \pi^-)$	$1/\sqrt{2}$	$1/\sqrt{2}$
$\mathcal{BR}(B^- \rightarrow K^{*-} K^0)$	1.0	0.
$\mathcal{BR}(B^- \rightarrow K^{*0} K^-)$	0.	1.0
$\mathcal{BR}(B^- \rightarrow \Phi \pi^-)$	0.	0.
$\mathcal{BR}(B^- \rightarrow \rho^- \pi^0)$	$-1/\sqrt{2}$	$1/\sqrt{2}$
$\mathcal{BR}(\bar{B}^0 \rightarrow \rho^0 \bar{K}^0)$	$-1/\sqrt{2}$	0.
$\mathcal{BR}(\bar{B}^0 \rightarrow \omega \bar{K}^0)$	$1/\sqrt{2}$	0.
$\mathcal{BR}(\bar{B}^0 \rightarrow \rho^+ K^-)$	1.0	0.
$\mathcal{BR}(\bar{B}^0 \rightarrow K^{*-} \pi^+)$	0.	1.0
$\mathcal{BR}(B^- \rightarrow K^{*-} \pi^0)$	0.	$1/\sqrt{2}$
$\mathcal{BR}(\bar{B}^0 \rightarrow \Phi \bar{K}^0)$	0.	1.0
$\mathcal{BR}(B^- \rightarrow \bar{K}^{*0} \pi^-)$	0.	1.0
$\mathcal{BR}(B^- \rightarrow \rho^0 K^-)$	$1/\sqrt{2}$	0.
$\mathcal{BR}(B^- \rightarrow \rho^- \bar{K}^0)$	1.0	0.
$\mathcal{BR}(B^- \rightarrow \omega K^-)$	$1/\sqrt{2}$	0.
$\mathcal{BR}(B^- \rightarrow \Phi K^-)$	0.	1.0
$\mathcal{BR}(\bar{B}^0 \rightarrow \bar{K}^{*0} \eta)$	-0.665	0.469
$\mathcal{BR}(B^- \rightarrow K^{*-} \eta)$	-0.665	0.469

TABLE VIII. Flavor- $SU(3)$  Clebsch-Gordan coefficient for long distance penguin-like contributions. Notice that the channel  $B^- \rightarrow \Phi \pi^-$  vanishes due to OZI rule.

In practice, to the amplitudes described in the appendices we add the long distance amplitudes, given by:

$$\mathcal{A}^{\text{LD}}(B \rightarrow PV) = \frac{G_F}{\sqrt{2}} m_B^2 \lambda'_c (Cl^P \mathcal{A}^P + Cl^V \mathcal{A}^V) \quad (24)$$

for the non strange channels and

$$\mathcal{A}^{\text{LD}}(B \rightarrow PV) = \frac{G_F}{\sqrt{2}} m_B^2 \lambda_c (Cl^P \mathcal{A}^P + Cl^V \mathcal{A}^V) \quad (25)$$

for the strange channels. In equations (24) and (25),  $\mathcal{A}^P$  and  $\mathcal{A}^V$  are two complex numbers which are fitted in the global fit of scenario 2 and  $Cl^P$  and  $Cl^V$  are the flavor- $SU(3)$  Clebsch-Gordan coefficients which are given in table VIII. For both channels containing the  $\eta$  we have used the formulae

$$Cl^V = \frac{\cos\theta_8}{\sqrt{6}} - \frac{\sin\theta_0}{\sqrt{3}} \quad Cl^P = -2 \frac{\cos\theta_8}{\sqrt{6}} - \frac{\sin\theta_0}{\sqrt{3}} \quad (26)$$

with  $\theta_0 = -9.1^\circ$  and  $\theta_8 = -22.2^\circ$ .

The fit with long distance penguin contributions is presented in table VI under the label “Scenario 2”. The agreement with experiment is improved, it should be so, but not in such a fully convincing manner. The goodness of the fit is about 8 % which implies that this model is not excluded by experiment. However a look at table V shows that several fitted parameters are still stuck at the end of the allowed range of variation. In particular  $\rho_A = 1$  means that the uncalculable subleading contribution to QCDF is again stretched to its extreme.

Finally the fitted complex numbers which fix the size of the long distance penguin contribution (last four lines in table V) are small. To make this statement quantitative, assuming the long distance amplitude were alone, the values for  $\mathcal{A}^P$  and  $\mathcal{A}^V$  in table VI correspond to branching ratios which reach at their maximum  $6 \times 10^{-6}$  but are more generally in the vicinity of  $2 \times 10^{-6}$ . In part, this is due to the fact that, if some strange channels want a large non-perturbative contribution to increase their branching ratios, some other strange channels and particularly the  $B \rightarrow K\phi$  channels which are in good agreement with QCDF cannot accept the addition of a too large non-perturbative penguin contribution. This last point should be stressed: if the strange channels show a general tendency to be underestimated by QCDF, there is the striking exception of the  $\bar{s}s\bar{s}$  channels which agree very well with QCDF and make the case for charming penguins rather difficult.

## VI. CONCLUSION

We have made a global fit according to QCD factorisation of published experimental data concerning charmless  $B \rightarrow PV$  decays including CP asymmetries. We have only excluded from the fit the channels containing the  $\eta'$  meson. Our conclusion is that it is impossible to reach a good fit. As can be seen in the scenario 1 of table VI, the reasons of this failure is that the branching ratios for the strange channels are predicted significantly smaller than experiment except for the  $B \rightarrow \phi K$  channels, and in table VII it can be seen that the direct CP asymmetry of  $\bar{B} \rightarrow \rho^+ \pi^-$  is predicted very small while experiment gives it very large but only two sigmas from zero. Not only is the “goodness of the fit” smaller than .1 %, but the fitted parameters show a tendency to evade the allowed domain of QCD factorisation. One might wonder if we were not too strict in imposing the same scale  $\mu$  in all terms since the value of  $\mu$ , representing the effect of unknown higher order corrections, could be different in different classes of channels <sup>††</sup>. We have performed several tests relaxing this unicity of  $\mu$  and concluded that it affected very little the outcome of our fit.

For the sake of comparison with the authors of ref. [36] we have tried a fit without the channels containing a  $K^*$ . The result improves significantly. The only lesson we can receive from this is that one must look carefully at the evolution of the experimental results, many of them being recent, before drawing a final conclusion.

Both the small predicted branching ratios of the strange channels and the small predicted direct CP asymmetries in the non strange channels could be blamed on too small  $P$  amplitudes with too small “strong phases” relatively to the  $T$  amplitudes. We have therefore tried the addition of two “charming penguin” inspired long distance complex amplitudes combined, in order to make the model predictive enough, with exact flavor- $SU(3)$  and OZI rule. This fit is better than the pure QCDF one: with a goodness of the fit of about 8 % the model is not excluded by experiment. But the parameters show again a tendency to reach the limits of the allowed

---

<sup>††</sup>We thank Gerhard Buchalla for raising this question.

domain and the best fit gives rather small value to the long distance contribution. The latter fact is presumably due to the  $B \rightarrow \phi K$  which are well predicted by QCDF and thus deliver a message which contradicts the other strange channels. This seems to be the reason of the moderate success of our “charming penguin” inspired model.

Altogether, the present situation is unpleasant. QCDF seems to be unable to comply to experiment. QCDF implemented by an ad-hoc long distance model is not fully convincing. No clear hint for the origin of this problem is provided by the total set of experimental data. PQCD, also called  $k_T$  factorisation, would predict larger direct CP asymmetries, but we do not know if their sign would fit experiment neither if an overall agreement of the branching ratios with data can be achieved.

Maybe however, the coming experimental data will move enough to resolve, at least partly, this discrepancy. We would like to insist on the crucial importance of direct CP asymmetries in non-strange channels. If they confirm the tendency to be large, this would make the case for QCDF really difficult.

Finally we do not know yet the answer to our initial question: are we in a good position to study the unitarity-triangle angle  $\alpha$  from indirect CP asymmetries thanks to small penguins. If experimental data evolve so as to provide a better support to QCDF, one could become bold enough to use it in estimating  $\alpha$  and this would reduce the errors. Else, only model-independant bounds [45] could be used but they are not very constraining in part because of discrete ambiguities.

## ACKNOWLEDGEMENTS

We are grateful to Gerhard Buchalla for useful discussions on various aspects of this work. A. S. S. would like to thank PROCOPE 2002 and DESY for financial support. We thank André Gaidot, Alain Le Yaouanc, Lluis Oliver, Jean-Claude Raynal and Christophe Yèche for several enlightening discussions which initiated this work as well as Sébastien Descotes at a later stage.

## APPENDIX

### APPENDIX A: THE DECAY AMPLITUDES FOR $B \rightarrow PV$

Following ref. [32], we give the decay amplitudes for the following  $B \rightarrow PV$  decay processes:

#### (1) $b \rightarrow d$ processes:

$$\mathcal{A}(\overline{B}^0 \rightarrow \rho^- \pi^+) = \frac{G_F}{\sqrt{2}} m_B^2 f_\rho F_1^{B \rightarrow \pi}(m_\rho^2) \left\{ \lambda'_u a_1 + (\lambda'_u + \lambda'_c) [a_4 + a_{10}] \right\}. \quad (\text{A1})$$

$$\mathcal{A}(\overline{B}^0 \rightarrow \rho^+ \pi^-) = \frac{G_F}{\sqrt{2}} m_B^2 f_\pi A_0^{B \rightarrow \rho}(m_\pi^2) \left\{ \lambda'_u a_1 + (\lambda'_u + \lambda'_c) [a_4 + a_{10} - r_\chi^\pi (a_6 + a_8)] \right\}. \quad (\text{A2})$$

$$\begin{aligned} \mathcal{A}(\overline{B}^0 \rightarrow \pi^0 \rho^0) = & -\frac{G_F}{2\sqrt{2}} m_B^2 \left( f_\pi A_0^{B \rightarrow \rho}(m_\pi^2) \left\{ \lambda'_u a_2 - (\lambda'_u + \lambda'_c) \left[ a_4 - \frac{1}{2} a_{10} - r_\chi^\pi (a_6 - \frac{1}{2} a_8) + \frac{3}{2} (a_7 - a_9) \right] \right\} \right. \\ & \left. + f_\rho F_1^{B \rightarrow \pi}(m_\rho^2) \left\{ \lambda'_u a_2 - (\lambda'_u + \lambda'_c) [a_4 - \frac{1}{2} a_{10} - \frac{3}{2} (a_7 + a_9)] \right\} \right). \end{aligned} \quad (\text{A3})$$

$$\begin{aligned} \mathcal{A}(B^- \rightarrow \pi^- \rho^0) = & \frac{G_F}{2} m_B^2 \left( f_\pi A_0^{B \rightarrow \rho}(m_\pi^2) \left\{ \lambda'_u a_1 + (\lambda'_u + \lambda'_c) [a_4 + a_{10} - r_\chi^\pi (a_6 + a_8)] \right\} \right. \\ & \left. + f_\rho F_1^{B \rightarrow \pi}(m_\rho^2) \left\{ \lambda'_u a_2 + (\lambda'_u + \lambda'_c) [-a_4 + \frac{1}{2} a_{10} + \frac{3}{2} (a_7 + a_9)] \right\} \right). \end{aligned} \quad (\text{A4})$$

$$\begin{aligned} \mathcal{A}(B^- \rightarrow \rho^- \pi^0) = & \frac{G_F}{2} m_B^2 \left( f_\pi A_0^{B \rightarrow \rho}(m_\pi^2) \left\{ \lambda'_u a_2 + (\lambda'_u + \lambda'_c) \left[ -a_4 + \frac{1}{2} a_{10} - r_\chi^\pi (-a_6 + \frac{1}{2} a_8) + \frac{3}{2} (a_9 - a_7) \right] \right\} \right. \\ & \left. + f_\rho F_1^{B \rightarrow \pi}(m_\rho^2) \left\{ \lambda'_u a_1 + (\lambda'_u + \lambda'_c) [a_4 + a_{10}] \right\} \right). \end{aligned} \quad (\text{A5})$$

$$\begin{aligned} \mathcal{A}(B^- \rightarrow \pi^- \omega) = & \frac{G_F}{2} m_B^2 \left( f_\pi A_0^{B \rightarrow \omega}(m_\pi^2) \left\{ \lambda'_u a_1 + (\lambda'_u + \lambda'_c) [a_4 + a_{10} - r_\chi^\pi (a_6 + a_8)] \right\} \right. \\ & \left. + f_\omega F_1^{B \rightarrow \pi}(m_\omega^2) \left\{ \lambda'_u a_2 + (\lambda'_u + \lambda'_c) \left[ a_4 + 2(a_3 + a_5) + \frac{1}{2} (a_7 + a_9 - a_{10}) \right] \right\} \right). \end{aligned} \quad (\text{A6})$$

**(2)  $b \rightarrow s$  processes:**

$$\mathcal{A}(\overline{B}^0 \rightarrow K^{*-} \pi^+) = \frac{G_F}{\sqrt{2}} m_B^2 f_{K^*} F_1^{B \rightarrow \pi}(m_{K^*}^2) \left\{ \lambda_u a_1 + (\lambda_u + \lambda_c) [a_4 + a_{10}] \right\}. \quad (\text{A7})$$

$$\mathcal{A}(\overline{B}^0 \rightarrow K^- \rho^+) = \frac{G_F}{\sqrt{2}} m_B^2 f_K A_0^{B \rightarrow \rho}(m_K^2) \left\{ \lambda_u a_1 + (\lambda_u + \lambda_c) [a_4 + a_{10} - r_\chi^K (a_6 + a_8)] \right\}. \quad (\text{A8})$$

$$\begin{aligned} \mathcal{A}(\overline{B}^0 \rightarrow \overline{K}^0 \rho^0) = & \frac{G_F}{2} m_B^2 \left\{ f_K A_0^{B \rightarrow \rho}(m_{K^0}^2) (-\lambda_u - \lambda_c) \left[ a_4 - \frac{1}{2} a_{10} - r_\chi^K (a_6 - \frac{1}{2} a_8) \right] \right. \\ & \left. + f_\rho F_1^{B \rightarrow K}(m_\rho^2) \left[ \lambda_u a_2 + (\lambda_u + \lambda_c) \times \frac{3}{2} (a_9 + a_7) \right] \right\}. \end{aligned} \quad (\text{A9})$$

$$\begin{aligned} \mathcal{A}(B^- \rightarrow K^{*-} \pi^0) = & \frac{G_F}{2} m_B^2 \left[ f_\pi A_0^{B \rightarrow K^*}(m_\pi^2) \left\{ \lambda_u a_2 + (\lambda_u + \lambda_c) \times \frac{3}{2} (a_9 - a_7) \right\} \right. \\ & \left. + f_{K^*} F_1^{B \rightarrow \pi}(m_{K^*}^2) \{ \lambda_u a_1 + (\lambda_u + \lambda_c) (a_4 + a_{10}) \} \right]. \end{aligned} \quad (\text{A10})$$

$$\begin{aligned} \mathcal{A}(B^- \rightarrow K^- \rho^0) = & \frac{G_F}{2} m_B^2 \left[ f_K A_0^{B \rightarrow \rho}(m_K^2) \{ \lambda_u a_1 + (\lambda_u + \lambda_c) [a_4 + a_{10} - r_\chi^K (a_6 + a_8)] \} \right. \\ & \left. + f_\rho F_1^{B \rightarrow K}(m_\rho^2) \left\{ \lambda_u a_2 + (\lambda_u + \lambda_c) \times \frac{3}{2} (a_9 + a_7) \right\} \right]. \end{aligned} \quad (\text{A11})$$

$$\begin{aligned} \mathcal{A}(\overline{B}^0 \rightarrow \overline{K}^0 \omega) = & \frac{G_F}{2} m_B^2 \left( f_K A_0^{B \rightarrow \omega}(m_{K^0}^2) (\lambda_u + \lambda_c) \left[ a_4 - \frac{1}{2} a_{10} - r_\chi^K (a_6 - \frac{1}{2} a_8) \right] \right. \\ & \left. + f_\omega F_1^{B \rightarrow K}(m_\omega^2) \left\{ \lambda_u a_2 + (\lambda_u + \lambda_c) \left[ 2(a_3 + a_5) + \frac{1}{2} (a_9 + a_7) \right] \right\} \right). \end{aligned} \quad (\text{A12})$$

$$\begin{aligned} \mathcal{A}(B^- \rightarrow K^- \omega) = & \frac{G_F}{2} m_B^2 \left[ f_K A_0^{B \rightarrow \omega}(m_K^2) \{ \lambda_u a_1 + (\lambda_u + \lambda_c) (a_4 + a_{10} - r_\chi^K (a_6 + a_8)) \} \right. \\ & \left. + f_\omega F_1^{B \rightarrow K}(m_\omega^2) \left\{ \lambda_u a_2 + (\lambda_u + \lambda_c) \left( 2(a_3 + a_5) + \frac{1}{2} (a_9 + a_7) \right) \right\} \right]. \end{aligned} \quad (\text{A13})$$

$$\begin{aligned} \mathcal{A}(B^- \rightarrow K^{*-} \eta^{(\prime)}) = & \frac{G_F}{\sqrt{2}} m_B^2 \left( f_{K^*} F_1^{B \rightarrow \eta^{(\prime)}}(m_K^2) \{ \lambda_u a_1 + (\lambda_u + \lambda_c) (a_4 + a_{10}) \} + f_{\eta^{(\prime)}}^u A_0^{B \rightarrow K^*}(m_{\eta^{(\prime)}}^2) \right. \\ & \times \left\{ \lambda_u a_2 + \lambda_c a_2 \frac{f_{\eta^{(\prime)}}^c}{f_{\eta^{(\prime)}}^u} + (\lambda_u + \lambda_c) \left[ 2(a_3 - a_5) + \frac{1}{2} (a_9 - a_7) + r_\chi^{\eta^{(\prime)}} (a_6 - \frac{1}{2} a_8) \right. \right. \\ & \left. \left. + (a_3 - a_5 + a_9 - a_7) \frac{f_{\eta^{(\prime)}}^c}{f_{\eta^{(\prime)}}^u} + \left( a_3 - a_5 - \frac{1}{2} (a_9 - a_7) + a_4 - \frac{1}{2} a_{10} - r_\chi^{\eta^{(\prime)}} (a_6 - \frac{1}{2} a_8) \right) \frac{f_{\eta^{(\prime)}}^s}{f_{\eta^{(\prime)}}^u} \right] \right\}. \end{aligned} \quad (\text{A14})$$

$$\begin{aligned} \mathcal{A}(\overline{B}^0 \rightarrow \overline{K}^{*0} \eta^{(\prime)}) = & \frac{G_F}{\sqrt{2}} m_B^2 \left( f_{K^*} F_1^{B \rightarrow \eta^{(\prime)}}(m_K^2) (\lambda_u + \lambda_c) \left[ a_4 - \frac{1}{2} a_{10} \right] + f_{\eta^{(\prime)}}^u A_0^{B \rightarrow K^*}(m_{\eta^{(\prime)}}^2) \right. \\ & \times \left\{ \lambda_u a_2 + \lambda_c a_2 \frac{f_{\eta^{(\prime)}}^c}{f_{\eta^{(\prime)}}^u} + (\lambda_u + \lambda_c) \left[ 2(a_3 - a_5) + \frac{1}{2} (a_9 - a_7) + r_\chi^{\eta^{(\prime)}} (a_6 - \frac{1}{2} a_8) + \right. \right. \\ & \left. \left. + (a_3 - a_5 + a_9 - a_7) \frac{f_{\eta^{(\prime)}}^c}{f_{\eta^{(\prime)}}^u} + \left( a_3 - a_5 - \frac{1}{2} (a_9 - a_7) + a_4 - \frac{1}{2} a_{10} - r_\chi^{\eta^{(\prime)}} (a_6 - \frac{1}{2} a_8) \right) \frac{f_{\eta^{(\prime)}}^s}{f_{\eta^{(\prime)}}^u} \right] \right\}. \end{aligned} \quad (\text{A15})$$

$$\text{with } r_\chi^{\eta^{(\prime)}} = \frac{2m_{\eta^{(\prime)}}^2}{(m_b + m_s)(m_s + m_s)}.$$

**(3) Pure penguin processes:**

$$\mathcal{A}(B^- \rightarrow \pi^- \bar{K}^{*0}) = \frac{G_F}{\sqrt{2}} m_B^2 f_{K^*} F_1^{B \rightarrow \pi}(m_{K^*}^2) (\lambda_u + \lambda_c) \left[ a_4 - \frac{1}{2} a_{10} \right]. \quad (\text{A16})$$

$$\mathcal{A}(B^- \rightarrow \rho^- \bar{K}^0) = \frac{G_F}{\sqrt{2}} m_B^2 f_K A_0^{B \rightarrow \rho}(m_{K^0}^2) (\lambda_u + \lambda_c) \left[ a_4 - \frac{1}{2} a_{10} - r_\chi^K (a_6 - \frac{1}{2} a_8) \right]. \quad (\text{A17})$$

$$\mathcal{A}(B^- \rightarrow K^- K^{*0}) = \frac{G_F}{\sqrt{2}} m_B^2 f_{K^*} F_1^{B \rightarrow K}(m_{K^*}^2) (\lambda'_u + \lambda'_c) \left[ a_4 - \frac{1}{2} a_{10} \right]. \quad (\text{A18})$$

$$\mathcal{A}(B^- \rightarrow K^{*-} K^0) = \frac{G_F}{\sqrt{2}} m_B^2 f_K A_0^{B \rightarrow K^*}(m_{K^0}^2) (\lambda'_u + \lambda'_c) \left[ a_4 - \frac{1}{2} a_{10} - r_\chi^K (a_6 - \frac{1}{2} a_8) \right]. \quad (\text{A19})$$

$$\mathcal{A}(B^- \rightarrow \pi^- \phi) = -\frac{G_F}{2} m_B^2 f_\phi F_1^{B \rightarrow \pi}(m_\phi^2) (\lambda'_u + \lambda'_c) \left[ a_3 + a_5 - \frac{1}{2} (a_7 + a_9) \right]. \quad (\text{A20})$$

$$\begin{aligned} \mathcal{A}(B^- \rightarrow K^- \phi) &= \mathcal{A}(\bar{B}^0 \rightarrow \bar{K}^0 \phi) \\ &= \frac{G_F}{\sqrt{2}} m_B^2 f_\phi F_1^{B \rightarrow K}(m_\phi^2) (\lambda_u + \lambda_c) \left[ a_3 + a_4 + a_5 - \frac{1}{2} (a_7 + a_9 + a_{10}) \right]. \end{aligned} \quad (\text{A21})$$

**APPENDIX B: THE ANNIHILATION AMPLITUDES FOR  $B \rightarrow PV$**

We give in this section the following annihilation amplitudes for  $B \rightarrow PV$  already given in ref. [35] but with different notations:

**(1)  $b \rightarrow d$  processes:**

$$\begin{aligned} \mathcal{A}^a(\bar{B}^0 \rightarrow \pi^- \rho^+) &= \frac{G_F}{\sqrt{2}} f_B f_\pi f_\rho \left\{ \lambda'_u b_1(\rho^+, \pi^-) + (\lambda'_u + \lambda'_c) \left[ b_3(\pi^-, \rho^+) + b_4(\rho^+, \pi^-) + b_4(\pi^-, \rho^+) \right. \right. \\ &\quad \left. \left. - \frac{1}{2} b_3^{ew}(\pi^-, \rho^+) + b_4^{ew}(\rho^+, \pi^-) - \frac{1}{2} b_4^{ew}(\pi^-, \rho^+) \right] \right\}. \end{aligned} \quad (\text{B1})$$

$$\begin{aligned} \mathcal{A}^a(\bar{B}^0 \rightarrow \pi^+ \rho^-) &= \frac{G_F}{\sqrt{2}} f_B f_\pi f_\rho \left\{ \lambda'_u b_1(\pi^+, \rho^-) + (\lambda'_u + \lambda'_c) \left[ b_3(\rho^-, \pi^+) + b_4(\pi^+, \rho^-) + b_4(\rho^-, \pi^+) \right. \right. \\ &\quad \left. \left. - \frac{1}{2} b_3^{ew}(\rho^-, \pi^+) + b_4^{ew}(\pi^+, \rho^-) - \frac{1}{2} b_4^{ew}(\rho^-, \pi^+) \right] \right\}. \end{aligned} \quad (\text{B2})$$

$$\begin{aligned} \mathcal{A}^a(\bar{B}^0 \rightarrow \pi^0 \rho^0) &= \frac{G_F}{2\sqrt{2}} f_B f_\pi f_\rho \left\{ \lambda'_u \left[ b_1(\rho^0, \pi^0) + b_1(\pi^0, \rho^0) \right] \right. \\ &\quad \left. + (\lambda'_u + \lambda'_c) \left[ b_3(\rho^0, \pi^0) + b_3(\pi^0, \rho^0) + 2b_4(\pi^0, \rho^0) + 2b_4(\rho^0, \pi^0) \right. \right. \\ &\quad \left. \left. + \frac{1}{2} \left( -b_3^{ew}(\rho^0, \pi^0) - b_3^{ew}(\pi^0, \rho^0) + b_4^{ew}(\pi^0, \rho^0) + b_4^{ew}(\rho^0, \pi^0) \right) \right] \right\}. \end{aligned} \quad (\text{B3})$$

$$\begin{aligned} \mathcal{A}^a(B^- \rightarrow \pi^- \rho^0) &= \frac{G_F}{2} f_B f_\pi f_\rho \left\{ \lambda'_u \left[ b_2(\pi^-, \rho^0) - b_2(\rho^0, \pi^-) \right] \right. \\ &\quad \left. + (\lambda'_u + \lambda'_c) \left[ b_3(\pi^-, \rho^0) - b_3(\rho^0, \pi^-) + b_3^{ew}(\pi^-, \rho^0) - b_3^{ew}(\rho^0, \pi^-) \right] \right\}. \end{aligned} \quad (\text{B4})$$

$$\begin{aligned} \mathcal{A}^a(B^- \rightarrow \pi^0 \rho^-) &= \frac{G_F}{2} f_B f_\pi f_\rho \left\{ \lambda'_u \left[ b_2(\rho^-, \pi^0) - b_2(\pi^0, \rho^-) \right] \right. \\ &\quad \left. + (\lambda'_u + \lambda'_c) \left[ b_3(\rho^-, \pi^0) - b_3(\pi^0, \rho^-) + b_3^{ew}(\rho^-, \pi^0) - b_3^{ew}(\pi^0, \rho^-) \right] \right\}. \end{aligned} \quad (\text{B5})$$

$$\begin{aligned} \mathcal{A}^a(B^- \rightarrow \pi^- \omega) &= \frac{G_F}{2} f_B f_\pi f_\omega \left\{ \lambda'_u \left[ b_2(\pi^-, \omega) + b_2(\omega, \pi^-) \right] \right. \\ &\quad \left. + (\lambda'_u + \lambda'_c) \left[ b_3(\pi^-, \omega) + b_3(\omega, \pi^-) + b_3^{ew}(\pi^-, \omega) + b_3^{ew}(\omega, \pi^-) \right] \right\}. \end{aligned} \quad (\text{B6})$$

**(2)  $b \rightarrow s$  processes:**

$$\mathcal{A}^a(\overline{B}^0 \rightarrow \pi^+ K^{*-}) = \frac{G_F}{\sqrt{2}} f_B f_\pi f_{K^*} \left\{ (\lambda_u + \lambda_c) \left[ b_3(K^{*-}, \pi^+) - \frac{1}{2} b_3^{ew}(K^{*-}, \pi^+) \right] \right\}. \quad (\text{B7})$$

$$\mathcal{A}^a(\overline{B}^0 \rightarrow K^- \rho^+) = \frac{G_F}{\sqrt{2}} f_B f_K f_\rho \left\{ (\lambda_u + \lambda_c) \left[ b_3(K^-, \rho^+) - \frac{1}{2} b_3^{ew}(K^-, \rho^+) \right] \right\}. \quad (\text{B8})$$

$$\mathcal{A}^a(\overline{B}^0 \rightarrow \overline{K}^0 \rho^0) = -\frac{G_F}{2} f_B f_K f_\rho \left\{ (\lambda_u + \lambda_c) \left[ b_3(\overline{K}^0, \rho^0) - \frac{1}{2} b_3^{ew}(\overline{K}^0, \rho^0) \right] \right\}. \quad (\text{B9})$$

$$\mathcal{A}^a(\overline{B}^0 \rightarrow \overline{K}^0 \omega) = \frac{G_F}{2} f_B f_K f_\omega \left\{ (\lambda_u + \lambda_c) \left[ b_3(\overline{K}^0, \omega) - \frac{1}{2} b_3^{ew}(\overline{K}^0, \omega) \right] \right\}. \quad (\text{B10})$$

$$\mathcal{A}^a(B^- \rightarrow K^- \omega) = \frac{G_F}{2} f_B f_K f_\omega \left\{ \lambda_u b_2(K^-, \omega) + (\lambda_u + \lambda_c) \left[ b_3(K^-, \omega) + b_3^{ew}(K^-, \omega) \right] \right\}. \quad (\text{B11})$$

$$\mathcal{A}^a(B^- \rightarrow \pi^0 K^{*-}) = \frac{G_F}{2} f_B f_\pi f_{K^*} \left\{ \lambda_u b_2(K^{*-}, \pi^0) + (\lambda_u + \lambda_c) \left[ b_3(K^{*-}, \pi^0) + b_3^{ew}(K^{*-}, \pi^0) \right] \right\}. \quad (\text{B12})$$

$$\mathcal{A}^a(B^- \rightarrow K^- \rho^0) = \frac{G_F}{2} f_B f_K f_\rho \left\{ \lambda_u b_2(K^-, \rho^0) + (\lambda_u + \lambda_c) \left[ b_3(K^-, \rho^0) + b_3^{ew}(K^-, \rho^0) \right] \right\}. \quad (\text{B13})$$

$$\begin{aligned} \mathcal{A}^a(\overline{B}^0 \rightarrow \eta^{(\prime)} \overline{K}^{*0}) = \frac{G_F}{\sqrt{2}} f_B f_{\eta^{(\prime)}}^u f_{K^*} \left\{ (\lambda_u + \lambda_c) \left[ b_3(\overline{K}^{*0}, \eta^{(\prime)}) \right. \right. \\ \left. \left. - \frac{1}{2} b_3^{ew}(\overline{K}^{*0}, \eta^{(\prime)}) + \frac{f_{\eta^{(\prime)}}^s}{f_{\eta^{(\prime)}}^u} \left( b_3(\eta^{(\prime)}, \overline{K}^{*0}) - \frac{1}{2} b_3^{ew}(\eta^{(\prime)}, \overline{K}^{*0}) \right) \right] \right\}. \end{aligned} \quad (\text{B14})$$

$$\begin{aligned} \mathcal{A}^a(B^- \rightarrow \eta^{(\prime)} K^{*-}) = \frac{G_F}{\sqrt{2}} f_B f_{\eta^{(\prime)}}^u f_{K^*} \left\{ \lambda_u \left[ b_2(K^{*-}, \eta^{(\prime)}) + \frac{f_{\eta^{(\prime)}}^s}{f_{\eta^{(\prime)}}^u} b_2(\eta^{(\prime)}, K^{*-}) \right] \right. \\ \left. + (\lambda_u + \lambda_c) \left[ b_3(K^{*-}, \eta^{(\prime)}) + b_3^{ew}(K^{*-}, \eta^{(\prime)}) + \frac{f_{\eta^{(\prime)}}^s}{f_{\eta^{(\prime)}}^u} \left( b_3(\eta^{(\prime)}, K^{*-}) + b_3^{ew}(\eta^{(\prime)}, K^{*-}) \right) \right] \right\}. \end{aligned} \quad (\text{B15})$$

**(3) Pure penguin processes:**

$$\mathcal{A}^a(B^- \rightarrow \pi^- \overline{K}^{*0}) = \frac{G_F}{\sqrt{2}} f_B f_\pi f_{K^*} \left\{ \lambda_u b_2(\overline{K}^{*0}, \pi^-) + (\lambda_u + \lambda_c) \left[ b_3(\overline{K}^{*0}, \pi^-) + b_3^{ew}(\overline{K}^{*0}, \pi^-) \right] \right\}. \quad (\text{B16})$$

$$\mathcal{A}^a(B^- \rightarrow \overline{K}^0 \rho^-) = \frac{G_F}{\sqrt{2}} f_B f_K f_\rho \left\{ \lambda_u b_2(\overline{K}^0, \rho^-) + (\lambda_u + \lambda_c) \left[ b_3(\overline{K}^0, \rho^-) + b_3^{ew}(\overline{K}^0, \rho^-) \right] \right\}. \quad (\text{B17})$$

$$\mathcal{A}^a(B^- \rightarrow K^- K^{*0}) = \frac{G_F}{\sqrt{2}} f_B f_K f_{K^*} \left\{ \lambda'_u b_2(K^{*0}, K^-) + (\lambda'_u + \lambda'_c) \left[ b_3(K^{*0}, K^-) + b_3^{ew}(K^{*0}, K^-) \right] \right\}. \quad (\text{B18})$$

$$\mathcal{A}^a(B^- \rightarrow K^0 K^{*-}) = \frac{G_F}{\sqrt{2}} f_B f_K f_{K^*} \left\{ \lambda'_u b_2(K^0, K^{*-}) + (\lambda'_u + \lambda'_c) \left[ b_3(K^0, K^{*-}) + b_3^{ew}(K^0, K^{*-}) \right] \right\}. \quad (\text{B19})$$

$$\mathcal{A}^a(B^- \rightarrow \pi^- \phi) = \mathcal{A}^a(\overline{B}^0 \rightarrow \pi^0 \phi) = 0. \quad (\text{B20})$$

$$\mathcal{A}^a(B^- \rightarrow K^- \phi) = \frac{G_F}{\sqrt{2}} f_B f_K f_\phi \left\{ \lambda_u b_2(\phi, K^-) + (\lambda_u + \lambda_c) \left[ b_3(\phi, K^-) + b_3^{ew}(\phi, K^-) \right] \right\}. \quad (\text{B21})$$

$$\mathcal{A}^a(\overline{B}^0 \rightarrow \overline{K}^0 \phi) = \frac{G_F}{\sqrt{2}} f_B f_K f_\phi \left\{ (\lambda_u + \lambda_c) \left[ b_3(\phi, \overline{K}^0) - \frac{1}{2} b_3^{ew}(\phi, \overline{K}^0) \right] \right\}. \quad (\text{B22})$$

- 
- [1] B. Aubert, *et al.* (for the BABAR Collaboration), hep-ex/0107058.  
[2] Thomas Schietinger (for the BABAR Collaboration), in *Proceedings of the Lake Louise Winter Institute on Fundamental Interactions, Alberta, Canada, February 2001*, hep-ex/0105019.  
[3] B. Aubert, *et al.* (for the BABAR Collaboration), Phys. Rev. Lett. **87**, 151801 (2001) .  
[4] B. Aubert, *et al.* (for the BABAR Collaboration), hep-ex/0107037.  
[5] B. Aubert, *et al.* (for the BABAR Collaboration), hep-ex/0109007.  
[6] B. Aubert, *et al.* (for the BABAR Collaboration), hep-ex/0109006.

- [7] B. Aubert *et al.* [BABAR Collaboration], Phys. Rev. D **65**, 051101 (2002).
- [8] B. Aubert *et al.* [BABAR Collaboration], hep-ex/0206053.
- [9] B. Aubert *et al.* [BABAR Collaboration], hep-ex/0207068.
- [10] B. Aubert *et al.* (BaBar Collab.), Phys. Rev. Lett. **87**, 221802 (2001); A. Bevan (BaBar Collab.), talk presented at ICHEP2002, Amsterdam, Holland, 24-31 July 2002; P. Bloom (BaBar Collab.), talk at Meeting of the Division of Particles and Fields, American Physical Society, Williamsburg, Virginia, 24-28 May 2002.
- [11] B.C.K. Casey *et al.* (Belle Collab.), Phys. Rev. D **66**, 092002 (2002); R.S. Lu *et al.* (Belle Collab.), Phys. Rev. Lett. **89**, 191801 (2002); A. Gordon *et al.* (Belle Collab.), Phys. Lett. B **542**, 183 (2002); A. Garmash *et al.* [Belle Collaboration], Phys. Rev. D **65**, 092005 (2002); Chang (Belle Collab.), talk presented at ICHEP2002, Amsterdam, Holland, 24-31 July 2002; K.F. Chen (Belle Collab.), talk presented at ICHEP2002, Amsterdam, Holland, 24-31 July 2002; H.C. Huang (Belle Collab.), talk at 37th Rencontres de Moriond on Electroweak Interactions and Unified Theories, Les Arcs, France, 9-16 March 2002, to appear in the Proceedings.
- [12] A. Bozek (for the Belle Collaboration), in *Proceedings of the 4th International Conference on B Physics & CP Violation, Ise-Shima, Japan, February 2001*, hep-ex/0104041.
- [13] K. Abe, *et al.* (for the Belle Collaboration), Belle-CONF-0115 (2001), in *Proceedings of the XX International Symposium on Lepton & Photon Interactions at High Energies, July 23-28, 2001, Rome, Italy*.
- [14] H. Tajima (for the Belle Collaboration), hep-ex/0111037.
- [15] K. Abe, *et al.* (for the Belle Collaboration), hep-ex/0201007.
- [16] R. A. Briere, *et al.* (CLEO Collaboration), Phys. Rev. Lett. **86**, 3718 (2001).
- [17] C. P. Jessop, *et al.* (CLEO Collaboration), Phys. Rev. Lett. **85**, 2881 (2000).
- [18] M. Bishai, *et al.* (CLEO Collaboration), hep-ex/9908018.
- [19] S. J. Richichi, *et al.* (CLEO Collaboration), Phys. Rev. Lett. **85**, 520 (2000).
- [20] S. Chen, *et al.* (CLEO Collaboration), Phys. Rev. Lett. **85**, 525 (2000).
- [21] D. Cronin-Hennessy *et al.* (CLEO Collab.), Phys. Rev. Lett. **85**, 515 (2000); E. Eckhart *et al.* (CLEO Collab.), hep-ex/0206024.
- [22] M. Beneke, G. Buchalla, M. Neubert and C. T. Sachrajda, Phys. Rev. Lett. **83**, 1914 (1999); Nucl. Phys. B **591**, 313 (2000).
- [23] M. Beneke, G. Buchalla, M. Neubert and C. T. Sachrajda, Nucl. Phys. B **606**, 245 (2001).
- [24] C. Isola, M. Ladisa, G. Nardulli, T. N. Pham and P. Santorelli, Phys. Rev. D **65**, 094005 (2002).
- [25] M. Ciuchini, E. Franco, G. Martinelli, M. Pierini and L. Silvestrini, Phys. Lett. B **515**, 33 (2001).
- [26] C. W. Chiang, Phys. Rev. D **62**, 014017 (2000).
- [27] M. Ciuchini, R. Contino, E. Franco, G. Martinelli and L. Silvestrini, Nucl. Phys. B **512**, 3 (1998) [Erratum-ibid. B **531**, 656 (1998)].
- [28] M. Ciuchini, E. Franco, G. Martinelli and L. Silvestrini, hep-ph/9909530.
- [29] C. Isola, M. Ladisa, G. Nardulli, T. N. Pham and P. Santorelli, Phys. Rev. D **64**, 014029 (2001).
- [30] M. Ciuchini, E. Franco, G. Martinelli and L. Silvestrini, Nucl. Phys. B **501**, 271 (1997).
- [31] R. Aleksan, F. Buccella, A. Le Yaouanc, L. Oliver, O. Pene and J. C. Raynal, Phys. Lett. B **356**, 95 (1995).
- [32] A. Ali, G. Kramer and C. D. Lü, Phys. Rev. D **58**, 094009 (1998); Phys. Rev. D **59**, 014005 (1999).
- [33] G. Kramer, W. F. Palmer and H. Simma, Z. Phys. C **66**, 429 (1995).
- [34] M. Z. Yang and Y. D. Yang, Phys. Rev. D **62**, 114019 (2000).
- [35] D. s. Du, H. j. Gong, J. f. Sun, D. s. Yang and G. h. Zhu, Phys. Rev. D **65**, 094025 (2002).
- [36] D. s. Du, J. f. Sun, D. s. Yang and G. h. Zhu, hep-ph/0209233.
- [37] P. Ball and V. M. Braun, Phys. Rev. D **58**, 094016 (1998).
- [38] C. H. Chen, Y. Y. Keum and H. n. Li, Phys. Rev. D **64**, 112002 (2001).
- [39] Y. Y. Keum, hep-ph/0210127.
- [40] M. Nagashima and H. n. Li, hep-ph/0210173; Y. Y. Keum and H. n. Li, Phys. Rev. D **63**, 074006 (2001).
- [41] W. N. Cottingham, H. Mehrban and I. B. Whittingham, J. Phys. G **28**, 2843 (2002).
- [42] Y. Y. Keum, H. N. Li and A. I. Sanda, Phys. Lett. B **504**, 6 (2001); Phys. Rev. D **63**, 054008 (2001);
- [43] C. D. Lü, K. Ukai and M. Z. Yang, Phys. Rev. D **63**, 074009 (2001).
- [44] K. Hagiwara *et al.* [Particle Data Group Collaboration], Phys. Rev. D **66**, 010001 (2002).
- [45] Jérôme Charles, THESE, “Désintégration des mésons  $B$ ”, april 16 1999, Université Paris-Sud (France), see <http://tel.ccsd.cnrs.fr/>
- [46] F. James, MINUIT, CERN Program Library **D506**.